

# Chapter 15

## Multicellular Systems

### 15.1 The Morphogenesis of *Drosophila melanogaster*

The morphogenetic processes of *Drosophila melanogaster* (fruit fly) and *Homo sapiens* are homologous (i.e., similar) since they have been found to utilize closely related sets of genes in highly conserved manner. Because of easy genetic manipulations possible with insects relative to humans, most of our current knowledge about the molecular basis of animal morphogenesis has come from researches performed on *Drosophila*.

The life span of *Drosophila melanogaster* is about 30 days, and it takes 10 days for a fertilized *Drosophila* egg to become an *adult* fly. After fertilization, the *Drosophila* zygote begins mitosis (i.e., nuclear division), but cytokinesis (i.e., division of the cytoplasm) does not occur in the early stages of the embryo, resulting in a multinucleate cell called a *syncytium* (also called *syncytial blastoderm*). Because of the common cytoplasm shared by all the nuclei of the syncytium, morphogen (i.e., diffusible molecules regulating morphogenesis) gradients play a key role in controlling the pattern of transcription of individual nuclei. At the tenth nuclear division, the nuclei migrate to the periphery of the embryo, and at the thirteenth nuclear division, the 6,000–8,000 nuclei are partitioned into separate cells forming the *cellular blastoderm*. The embryogenesis, that is, the process of a fertilized egg to develop into an embryo, takes about 15 h in *Drosophila*.

Lécuyer et al. (2007) used the fluorescence *in situ* hybridization (FISH) technique to determine the localization in the embryo of approximately 25% of the mRNA encoded in the *Drosophila* genome. They found that the majority of sampled mRNAs (i.e., 71% of 3,370 genes, or 2,360 genes) are localized in the early embryo as illustrated in Fig. 15.1. Their study demonstrates that mRNA localization in *Drosophila* embryo is heterogeneous and suggests that such a distribution of mRNA in embryo may be a widespread biological phenomenon playing a fundamental role in organizing cellular architecture.

The patterns of distribution of mRNA molecules in cells measured with microarrays can be either spatial (Fig. 15.1) (Lécuyer et al. 2007) or temporal

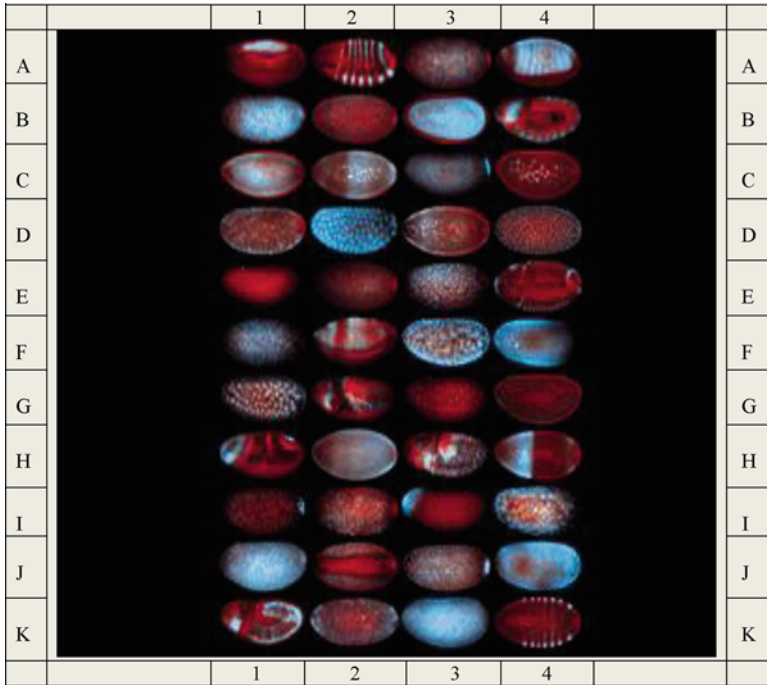
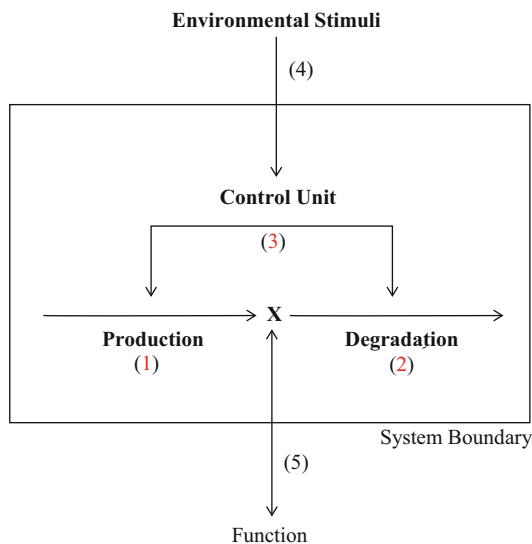


**Fig. 15.1** Asymmetric distribution of mRNA molecules in *Drosophila* visualized with fluorescent in situ hybridization (FISH) technique (Lécuyer et al. 2007). The mRNA molecules are depicted in *blue* and nuclei in *red*. There are a total of 44 embryo images in this figure in 11 rows and 4 columns. To identify individual images, rows are labeled with capital letters and the columns with Arabic numerals. Thus, Image A1 will designate the image on the first row and the first column, and Image K4 will designate the image on the last row and the last column, etc. (The embryo images were reproduced from Lécuyer et al. 2007 by permission of *Cell* obtained through Copyright Clearance Center)

(Figs. 12.1, 12.2, 12.3). Both the RNA distributions in *time* and *space* are expected to obey the *Triadic Control Principle* (TCP) described in Fig. 15.2. Just as the majority of workers in the field of DNA microarray technology in the past decade committed false-positive and false-negative errors in interpreting their data due to ignoring TCP (Ji et al. 2009a), so it can be predicted that researchers employing the FISH technique to measure spatial distributions of mRNA signals such as shown in Fig. 15.1 can make similar errors in interpreting their data if TCP is not taken into account. For example, if an mRNA signal was found to be high in the anterior region relative to the posterior region in a syncytial *Drosophila* blastoderm (e.g., see I3 in Fig. 15.1), the usual interpretation is that the transcription rate of the associated gene is higher in the anterior region than in the posterior region, or that the associated gene is *expressed* in the anterior region but not in the posterior region of the embryo (see Table 1 in Lécuyer et al. 2007). But, in the absence of independent data, it would be impossible to rule out the alternative possibility

**Fig. 15.2** A diagrammatic representation of the “triadic control principle” (TCP), also called “triadic control hypothesis” (TCH), or the “triadic control mechanism” (TCM). Please note that Processes 1, 2, and 3 are *internal* to the system (whence the notion of triadic control) and X is the *effector unit*. Process 4 is environmental input, and Process 5 is the environmental message-triggered function (or output) of the system immediately caused or effectuated by X



that the same observation may be the result of a decreased rate of transcript degradation in the anterior region of the embryo relative to the posterior region without any gradient in the transcription rate of the associated gene between these two regions. Adopting the first interpretation and inferring the associated gene to be responsible for the observed mRNA gradient thus can lead to a false-positive (or Type I) error if the alternative interpretation turns out to be true.

The structural elements forming the anterior-posterior axis in *Drosophila* are already put in place during egg formation (or oogenesis) before fertilization. Developing oocyte is polarized by mRNA molecules differentially bound to cytoskeletal elements (if the local mRNA concentration is determined predominantly by transcription and not by transcript degradation; see the Triadic Control Principle explained in Fig. 15.2). The genes coding for these mRNA molecules are called *maternal effect genes*. The differentially bound mRNA molecules get translated upon fertilization to form concentration gradients of the resulting proteins across the egg cytoplasm. *Bicoid* and *hunchback* are two maternal effect genes playing the most important roles in patterning anterior parts (head and thorax) of the *Drosophila* embryo, and *Nanos* and *Caudal* are maternal effect genes that are important in determining posterior abdominal segments of the embryo. Maternally synthesized *bicoid* mRNA molecules preferentially accumulate in the anterior end of developing *Drosophila* eggs, and *Nanos* mRNA accumulate at the posterior end of the eggs, resulting in oppositely directed gradients of *bicoid* and *nanos* mRNA molecules. When these mRNA molecules are translated into proteins, Bicoid and Nanos gradient are formed along the anterior-posterior axis. *Hunchback* and *caudal* mRNA molecules are evenly distributed throughout the interior of egg cells, but their protein products are distributed unevenly because (1) Bicoid protein inhibits the translation of *hunchback* mRNA and Nanos protein inhibits the translation of

the *hunchback* mRNA, and (2) Bicoid and Nanos proteins are unevenly distributed across the *Drosophila* egg.

The Bicoid, Hunchback, Nanos, and Caudal are transcription factors that regulate the transcription of gap genes such as *Krüppel*, *giant*, *tailless*, and *Knirps*. Gap genes are part of a larger family called the *segmentation genes* that determine the segmental body plan of the embryo along the anterior-posterior axis. They are called “gap genes” because their expression leads to the formation of gaps in the normal pattern of structure or the formation of broad bands in the embryo.

The maternal effect genes, including *bicoid* and *nanos*, are required during oogenesis. The transcripts or protein products of these genes are found in the egg at fertilization, and form morphogen gradients. The pair-rule genes divide the embryo into pairs of segments. These genes encode transcription factors that regulate the expression of the segment polarity genes, whose role is to set the anterior-posterior axis of each segment. The gap genes, pair-rule genes, and segment polarity genes are together called the segmentation genes, because they are involved in segment patterning.

The order of the expression of the set of genes, maternal effect genes, gap genes, pair-rule genes, and segment polarity genes leads to an increasingly differentiated and diversified *spatial compartmentation* of the volume occupied by the *Drosophila* embryo which in turn leads to increasing the “active” complexity of the embryo, “active” because such *compartmentations* would be impossible without dissipating free energy. The concepts of “active” and “passive” complexities were defined in Sect. 5.2.3. Therefore, it appears logical to define what may be referred to as “the active complexity of the embryo” (ACE) as the number of bits in the shortest string of symbols that describes the geometric compartmentation of an embryo, including the body segmentations:

$$\text{Active Complexity of the Embryo (ACE)} = \frac{\text{Algorithmic Complexity of the Geometric Compartments of the Embryo}}{\text{Geometric Volume of the Embryo}} \quad (15.1)$$

Once the concept of active complexity of embryo (ACE) is defined, it is simple to take the next logical step and define what may be called the “information density of the embryo” (IDE) as the ratio of ACE and the geometric volume of the embryo (GVE):

$$\text{Information Density of the Embryo (IDE)} = \frac{\text{Spatial Complexity of the Embryo (ACE)}}{\text{Geometric Volume of the Embryo (GVE)}} \quad (15.2)$$

It is important to differentiate the IDE from what may be called the “information density of the genome” (IDG), defined as the ratio of the algorithmic complexity of the nucleotide sequences of the genome over the geometric volume of the genomic DNA molecules, since embryo is dissipative structures (or dissipatons) and the genome, as defined here, would be an equilibrium structures (or equilibrons)

(Sect. 3.1). To use a familiar metaphor, embryos are akin to *audio music* and the genomes are akin to *sheet music*. Because the quality of audio music depends on many more factors (such as the artistic skills of the musician, the kinds of instruments employed, the environmental factor, etc.) than the quality of a sheet music, the information content of audio music is much greater than the information content of a sheet music. One characteristic of sheet music is that it can be handed down from one generation to another without any change. As evident in Fig. 15.1, both the genome and the volume of the *Drosophila* embryo remain more or less constant during most of the embryogenesis, but the algorithmic information content of the embryo (and hence the IDE) obviously increases as the *Drosophila* embryogenesis progresses. The genomic information density of a species tends to increase over generations (i.e., on the diachronic timescale, not on the synchronic timescale; see Sect. 14.4 and Fig. 14.3 for the definitions of “synchronic ” and “diachronic ” timescales), leading to Statement 15.3:

The information density of the genome increases with diachronic time; the information density of embryos increases with synchronic time. (15.3)

Statement 15.3 is consistent with the Law of Maximum Complexity, Statement 14.15, described in Sect. 14.3.

The transcription factors coded for by segmentation genes also regulate the *Law of Maximum Complexity*. These genes are located in *Drosophila* chromosome 3, and the order of the genes on the chromosome determines the order in which they are expressed along the anterior-posterior axis of the embryo. The Antennapedia group of homeotic selector genes includes *labial*, *antennapedia*, *sex combs reduced*, *deformed*, and *proboscipedia*. *Labial* and *deformed* genes are expressed in head segments (where their protein products activate the genes defining head features), and *sex-combs-reduced* and *antennapedia* genes encode the proteins that specify the properties of thoracic segments. In *Drosophila*, antennae and legs are created by the same program except a single transcription factor. When this transcription factor is mutated, the fly grows legs on its head in place of antennae, a phenomenon known as the *antennapedia mutation* (<http://zygote.swathmore.edu/droso4.html>).

The antennapedia homeodomain is a sequence-specific transcription factor from *Drosophila* encoded by the Antennapedia (*antp*) gene. The antennapedia homeodomain (Antp) is a member of a regulatory system that gives cells specific positions on the anterior-posterior axis of the organism. Antp aids in the control of cell development in the mesothorax segment in *Drosophila*. The homeobox domain (or homeodomain) binds DNA through a helix-turn-helix structural motif.

Homeobox genes (about 180 base pairs) were discovered in 1983, and the proteins they encode, the *homeodomain proteins* (~60 amino acid residues long) have been found to play important roles in the developmental processes of many multicellular organisms. They have been shown to play crucial roles in embryogenesis and have a wide phylogenetic distribution. Hundreds of homeobox genes have been described in baker's yeast, plants, and all animal phyla (Bürglin 1996).

## 15.2 The Role of DNA, RNA, and Protein Gradients in *Drosophila* Embryogenesis

At the syncytial blastodermal stage of *Drosophila* embryo (see K3 in Fig. 15.1), we can recognize three kinds of macromolecular gradients:

1. The *DNA gradients* high in the periphery of the embryo and low in its interior (as can be inferred from the RNA Images A2, B4, E4, and K4 in Fig. 15.1),
2. The *RNA gradients* along the anterior-posterior axes (see Images A4, C2, D3, F2, G2, H2, H4, J3, and K4), the dorsal-ventral axes (see Images A1, A2, and B4), and other directions (see Images E4, G2, H1, H3, I3, and K4), and
3. The *protein gradients* that can be inferred from RNA gradients since no RNA would be synthesized or degraded without the associated catalytic proteins or enzymes. Protein gradients must also be present to act as molecular transporters or motors (Chap. 8) responsible for generating DNA and/or RNA gradients.

A macromolecular gradient has two fundamental properties – (1) the property intrinsic to the macromolecule (hence to be referred to as the *intrinsic* or *single-molecule property*) and (2) the property arising from its being a part of a gradient (to be referred to as the *extrinsic* or *collective property*). Of course, any gradient can be of two distinct kinds – (1) the *spatial gradient* (more *here* than *there*) such as those asymmetric RNA localization images given in Fig. 15.1, and (2) the *temporal gradient* (more *now* than *before*) such as the RNA trajectories shown in Figs. 12.1 and 12.2a. The shape (i.e., the cooperative property of a macromolecule) of a gradient may be compared to an *audio music* and the intrinsic property of a macromolecule to a *sheet music*. In this analogy, the cellular genome is a master sheet music and the RNA and protein gradients are the audio music in two different media or channels having different effective ranges or fields of activity (see Row 3 in Table 15.1). Another way to characterize the roles of DNA, RNA, and protein gradients in an embryo is in terms of the concept of *molecular computing* or a *system of molecular computers* that are communicating with one another (to accomplish a common task) using the cell language (Sect. 6.1.2) mediated by intercellular protein messengers (see Row 5 in Table 15.1). Viewed in this manner, the RNA localization (or gradient) images such as displayed in Fig. 15.1 can be considered to represent an instantaneous computing activity (observed through the lens of RNA) that is being carried out by the *Drosophila* embryo as it develops toward an adult fruit fly.

## 15.3 The Triadic Control Principle (TCP)

The analysis of the genome-wide variations of the RNA levels in budding yeast undergoing glucose-galactose shift (see Sect. 12.3) strongly indicates that the intracellular concentration of RNA molecules is constantly *controlled* by the cell

**Table 15.1** The roles of DNA, RNA, and proteins in *Drosophila* embryogenesis

	DNA	RNA	Protein
1. <i>Average size</i> (arbitrary unit)	3	2	1
2. <i>Diffusibility</i> (arbitrary unit)	1	2	3
3. <i>Effective range of action</i>	(a) Nucleus	(a) Nucleus (b) Cytoplasm	(a) Nucleus (b) Cytoplasm (c) Extracellular space
4. <i>Catalytic activity</i>	No	Almost none	Yes
5. <i>Function</i>	Secondary memory (Sect. 11.2.6)	Primary memory (Sect. 11.2.6)	Soft transistor (Sect. 5.1.1)
	Optimal form for information reproduction	Optimal for information retrieval Molecular computing Cell language (Table 6.3)	Optimal form for energy transduction <sup>a</sup>

<sup>a</sup>From chemical to mechanical forms, i.e., conformons (Chap. 8)

to meet its needs by balancing the *rates of production* ( $V_P$ ) and the *rates of degradation* ( $V_D$ ) of RNA (see Steps 1 and 2 in Fig. 15.2). Depending on the needs of the cell, the concentrations of intracellular levels of specific RNA molecules are *actively maintained* at one of the following three dynamic states:

1. *Dynamic steady states* (when  $V_P = V_D$ ),
2. *Ascending states* (when  $V_P > V_D$ ), and
3. *Descending states* (when  $V_P < V_D$ ).

Recent evidence indicates that  $V_P$  and  $V_D$  are space- and time-dependent, often regulated by microRNAs (Makeyev and Maniatis 2008), thereby qualifying space- and time-dependent RNA levels as members of *dissipative structures* and, more specifically, members of IDSs or r-dissipatons (see Sect. 3.1.2).

The Triadic Control Principle (or Hypothesis) depicted in Fig. 15.2 is so called because of the existence of two opposing processes, 1 and 2, under the control of a third process, 3. The source of the control signals, or the agent of the cell control, is postulated to be the *cell itself* which is in constant communication with its neighbors and environment (by exchanging information carried by diffusible molecules or through local electric fields) and perform molecular computation under the guidance of DNA programs (sheet music). This postulate is consistent with or equivalent to the postulate that the cell is the smallest DNA-based molecular computer or *the Computon* (see Row 9 and Footnote 7 in Table 6.3) (Ji 1999a). The modifier, “triadic”, also implies (1) that there are three, and only three, classes of the processes underlying cell functions, namely, *production*, *degradation*, and

control of production and degradation, and (2) that there exists a hierarchy among these three processes:

$$\mathbf{Production} > \mathbf{Degradation} > \mathbf{Control} \quad (15.4)$$

where the symbol, “ $\mathbf{A} > \mathbf{B}$ ”, reads as “ $\mathbf{A}$  must precede  $\mathbf{B}$ ” or “ $\mathbf{A}$  is a prerequisite for  $\mathbf{B}$ ”. Scheme (15.4), when applied to Fig. 15.2, suggests (1) that  $\mathbf{X}$  must be produced before it can be degraded, and (2) that the production and degradation processes of  $\mathbf{X}$  must be in place before they can be controlled. This is reminiscent of a similar hierarchical relation that obtains among the three fundamental aspects of reality that Peirce referred to as Firstness, Secondness, and Thirdness (Sect. 6.2.2).

If the system under consideration is the cell, then the function of the cell is postulated to depend on the presence of a set  $\mathbf{X}$  of molecules and ions inside the cell. If the system under consideration is a subcellular compartment of a developing embryo such as the peripheral compartment of a syncytial blastoderm, then the function of such a compartment is thought to depend on the set  $\mathbf{X}$  of molecules and ions present in that compartment as a balance between their input into and output from the compartment. The concentrations or levels of the members of  $\mathbf{X}$  can be controlled by regulating their rates of *production* (or input) and *degradation* (or output). The vertical double-headed arrow indicates an identity relation. The horizontal arrows indicate irreversible processes driven by free energy dissipation. The numerals 1, 2, and 3 refer to the hierarchical relation shown in Inequality (15.4): Without 1, no 2; without 2, no 3. The source of the control signals is postulated to be the cell itself which communicate with its neighbors and environment as indicated above.

The nature of  $\mathbf{X}$  in Fig. 15.2 can be any material or physical entities controlled by the system under consideration, including activated genes, pre-mRNAs, mRNAs, nc-RNAs (Amaral et al. 2008, Mattick 2003, 2004), microRNAs (Hobert 2008, Makeyev and Maniatis 2008), small-molecular-weight entities such as glucose, ATP,  $P_i$ , NADH, and metal ions.  $\mathbf{X}$  need not be confined to the cell and can represent any material entities that play fundamental role in living systems such as blood level of hormones, glucose, and other metabolites, blood content of an organ, and the space- and time-dependent number of electrically active neurons in the brain, etc. In Table 15.2, the triadic control mechanism is applied to five different levels of biological organization, listing specific examples of the key components of the mechanism in a self-explanatory manner.

Enzymes may be viewed as one of the simplest material systems whose behaviors can be accounted for in terms of the *triadic control mechanism* depicted in Fig. 15.2. Enzymes can exist in at least two conformational states, *ground state* and *activated state* (characterized by the presence of sequence-specific conformational strains, i.e., *conformons*; see Figs. 11.30 and 14.7). The activated state of an enzyme is produced by substrate binding (Jencks 1975) and/or exergonic chemical reactions through generalized Franck–Condon mechanisms (see Fig. 8.1 and Sect. 11.4). The activated state of an enzyme is caused to *relax* back to its ground state when it performs a molecular work, be it catalysis (i.e., lowering the



**Table 15.2** The triadic control principle or mechanism applied to five levels of biological organization

Level	Production	X	Degradation	Control	Function
1. Subcellular	<i>Substrate binding, chemical reactions</i>	<i>Conformational strains<sup>a</sup> of biopolymers (Chap. 8)</i>	<i>Molecular work processes (e.g., catalysis, active transport)</i>	<i>Evolutionary information encoded in biopolymers (Sect. 11.3.3)</i>	<i>Time- and space-organized molecular processes (e.g., active transport, gene expression)</i>
	<i>Transcript-ion (transcriptosome)</i>	<i>RNAs (Chap. 12)</i>	<i>Transcript degradation (degradosome)</i>	<i>Biochemical signals (e.g., ATP, transcription factors, miRNAs)</i>	<i>Controlling metabolic activities (e.g., glycolysis, respiration, cell cycle, morphogenesis)</i>
	<i>Phosphorylation (kinases)</i>	<i>Phosphoproteins (e.g., activated enzymes)</i>	<i>Dephosphorylation (phosphatases)</i>	<i>Biochemical signals (e.g., cholesterol, cAMP, ATP)</i>	<i>Cell type-specific cell functions (production of key metabolites)</i>
2. Cellular	<i>Mitosis</i>	<i>Cells</i>	<i>Apoptosis</i>	<i>Intercellular messengers</i>	<i>Morphogenesis, organogenesis, carcinogenesis</i>
3. Tissue	<i>Blood inflow</i>	<i>Tissue blood content</i>	<i>Blood outflow</i>	<i>Hormones, nerve signals</i>	<i>Tissue-specific activities (e.g., brain activity)</i>
4. Organ (e.g., blood)	<i>Activation (e.g., by proteolysis)</i>	<i>Activated coagulation factors</i>	<i>Inactivation (by proteolysis, protein phosphatases)</i>	<i>Biochemical signals (e.g., from ruptured vessels)</i>	<i>Homeostasis of organ function (e.g., prevention of blood loss, i.e., hemostasis)</i>
5. Body	<i>Vasoconstriction, ↑cardiac output</i>	<i>Blood pressure</i>	<i>Vasodilation</i>	<i>Renin, angiotensin, aldosterone</i>	<i>Homeostasis of body perfusion (microcirculation)</i>
	<i>Activation (e.g., pleasurable stimuli)</i>	<i>Reward system activity</i>	<i>Deactivation (e.g., painful stimuli)</i>	<i>Habit, will</i>	<i>To promote the survival of individuals and species</i>

<sup>a</sup>Also called *conformons* (Chap. 8)

activation energy barrier) or exerting mechanical forces on its environment as in active transport (Sect. 8.5) or muscle contraction (Sect. 11.4). It is postulated that the *control information* that determines the number of conformations stored in an enzyme at any given time is encoded in the amino acid sequence of the enzyme which in turn determines the 3-dimensional shape of the enzyme under a given environmental condition. The function of the enzyme can be very broadly identified as the time- and space-organized biopolymer motions in the cell driven by exergonic chemical reactions, including not only molecular motor and pump functions but also basic catalysis such as covalent modification of substrates in solution.

## 15.4 The Synchronic vs. Diachronic System–Environment Interactions

In biology, we can recognize two distinct classes of *system-environment interactions* – (1) the *individual-environment interactions* (IEI) and (2) the *population-system interactions* (PEI) (see Row 1 in Table 15.3). IEI takes place over a

**Table 15.3** Synchronic and diachronic interactions between living systems and their environment

	Interactions	
	Synchronic	Diachronic
1. Systems	Individual organisms	Populations of organisms
2. Timescale (see Fig. 14.3)	Synchronic time (or <i>developmental time</i> )	Diachronic time (or <i>evolutionary time</i> )
3. Mechanisms of interactions	Force-mediated	Code-mediated
4. Principles obeyed	Laws of physics and chemistry (Secondness) <sup>a</sup>	Rules, codes, conventions (Thirdness) <sup>a</sup>
5. Fields	Molecular biology Chemical biology Epigenetics <sup>b</sup> (Synchronic biology) “Semantic biology” Cell biology ( <i>genomics</i> ) <sup>d</sup> Physiology “Evolutionary developmental biology (or EvoDevo)” “Developmental evolutionary biology” “Biosemiotics” <sup>e</sup> “Biogenergetics” <sup>f</sup>	Evolutionary biology Paleontology Genetics <sup>c</sup> (Diachronic biology)

<sup>a</sup>Related to the metaphysics of Peirce (see Sect. 6.2.1)

<sup>b</sup>The study of the effects of genes (other than their nucleotide sequences) on the phenotypes of individuals here and now

<sup>c</sup>The study of the effects of genes (i.e., their nucleotide sequences) of individuals on the phenotypes of their offspring

<sup>d</sup>Genomics is here defined as a combination of *epigenetics* and *genetics*

<sup>e</sup>The study of molecular signs (e.g., DNA, RNA, protein domains) in living systems (Sect. 6.2) (Sebeok 1990, Hoffmeyer 1996, Pattee 2008)

<sup>f</sup>The study of information (*gn-*) and energy (*-erg*) transductions in living systems (Ji 1985a, b)

relatively short timescale characteristic of individual life spans. In contrast, PEI occurs over a much longer timescale determined by the life span of populations or species. In Sect. 14.4, the former timescale was referred to as the *synchronic time* and the latter as the *diachronic time*. Hence, we may refer to IEI as *synchronic interactions* and PSI as the *diachronic interactions*. (For related discussions, see Sects. 2.6 and 4.5.)

Since all physical interactions are force-mediated, “physical interactions” and “synchronic interactions” are synonymous. There are four forces in nature – gravitational, electromagnetic, weak, and strong forces. The electromagnetic and weak forces are often combined as the electroweak force. Forces and energies are mathematically related to each other through the Second Law of Newtonian mechanics. Hence, “force-mediated” and “energy-mediated” can be used interchangeably. “Code-mediated” processes include all template-mediated processes in molecular and cell biology such as enzymic catalysis, replication, transcription, translation, receptor-mediated processes, and signal transduction in cell. These interactions are referred to as “diachronic interactions” because it takes a long time for the codes involved to develop and change, relative to the time it takes for a code to effectuate its functions, for example, as a template for copying activities.

What goes on in biological systems (i.e., enzymes, cells, tissues, animals, plants, etc.) obey the laws of physics and chemistry just as what goes on in nonbiological systems (e.g., rocks, machines, mountains, stars) do. But what distinguishes biological systems from nonbiological systems is the rules, codes, and conventions embodied in their boundary conditions or structures that harness or constrain the operation of the laws of physics and chemistry to accomplish their goals (see Row 4 in Table 15.3) (Bernstein 1967, Polanyi 1968, Pattee 1982, 2008). In other words, biology has two complementary aspects – law-governed and the rule-governed as pointed out by Pattee (182, 2008). Thus, it seems natural to divide biology into two branches, for example, *chemical biology* vs. *evolutionary biology* (see Row 5 in Table 15.3), depending on which of these two aspects of biology is being emphasized.

The dichotomy of the *law-governed* and *rule-governed* aspects of biology seems to be first recognized and has been systematically investigated by Pattee (1968, 1969, 1982, 1995, 1996, 2001, 2008) under the rubric of the *symbol-matter complementarity* during the past several decades. In (Ji 1999b), I referred to Pattee’s idea as the “von Neumann-Pattee principle of sign-matter complementarity” (VPPSMC) and pointed out the close theoretical relation existing between VPPSMC and the *information-energy complementarity* (IEC) or the *gnergy principle* (Sect. 2.3.2) formulated in the 1990s by extending Bohr’s principle of complementarity from quantum mechanics to biological phenomena including the operation of enzymes and molecular machines in living cells.

The *von Neumann-Pattee principle of sign-matter complementarity* (Pattee 1982, 2008, Ji 1999b) and the *information-energy complementarity* (Ji 1991, 1995) may be viewed as theoretical attempts to integrate both law-governed (i.e., *causal*) and rule-governed (i.e., *codal*) aspects of biology. A similar view has been expressed by Barbieri (2003, 2008a, b, c) who has been attempting to integrate the *syntactic* and *semantic* aspects of molecular biology under the umbrella of *biosemiotics* in

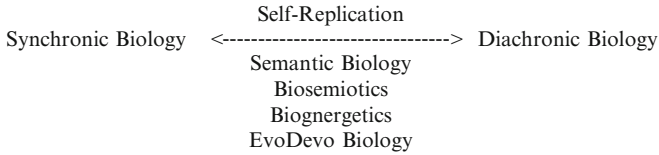


**Fig. 15.3** A classification of biology into three branches, two of which (synchronic and diachronic biologies) may be viewed as the complementary aspects of the third (semantic biology, biosemiotics, biognergetics, or EvoDevo biology). “Gnergy” is defined as the complementary union of information (gn-) and energy (-ergy) in analogy to light being the complementary union of waves and particles (Sect. 2.3.2), and “biognergetics” is the study of living processes viewed as being driven ultimately by *gnergy* or its discrete units, *gnergons*

agreement with (Hoffmeyer 1996, 2008, Pattee 2008). These theoretical developments coincide with the recent trend in experimental biology to integrate developmental biology and evolutionary biology, the trend often referred to as “evolutionary developmental biology” (EvoDevo) or “developmental evolutionary biology” (Carroll 2006, Kirschner and Gerhart 1998, West-Eberhard 1998, 2003). The newly emerging biology that attempts to integrate the traditionally independent developmental biology and evolutionary biology into a coherent system of knowledge and applications has been given numerous names by independent authors, some of which are listed in the last row of Table 15.3. The last row of Table 15.3 can also be represented diagrammatically as shown in Fig. 15.3, which highlights *self-replication* as the single most important process that glues together all of the three branches of biology.

## 15.5 The Dissipative Structure Theory of Morphogenesis

Morphogenesis is a dynamic process consisting of many component processes taking place in an organism coordinated in space and time. In short,

Morphogenesis is a dissipaton composed of a set of component dissipatons that are organized in space and time. (15.5)

The *dissipative structure-* or *dissipaton-based* approaches to cell biology described in the previous chapters (e.g., Sects. 3.1, 9.1, and 12.4) suggest the following set of generalizations as theoretical guides for formulating molecular mechanisms underlying morphogenesis:

1. There are two classes of structures in the Universe – equilibrium structures (*equilibrons*) and dissipative structures (*dissipatons*) (Sects. 3.1, 9.1). The key difference between *equilibrons* and *dissipatons* is that the former can exist without using up free energy while the latter requires continuous dissipation of free

**Table 15.4** Examples of *equilibrons* and *dissipatons* in the Universe

Size	Equilibrons	Dissipatons
Macroscopic	Chairs, tables, cold candle sticks, rocks, secondary memory of a computer	Candle flames, sounds, city traffic flow patterns, primary memory of a computer
Microscopic	X-ray structures of proteins, RNA and DNA, linear sequences of nucleotides in genes, molecular structures of ATP, NADH, and glucose	Membrane potentials, cytosolic gradients of ions and metabolites, spatiotemporal patterns of changes in RNA levels in cells and embryos (Figs. 9.1, 15.1)

energy for their existence. Thus, anything that disappears when free energy supply is blocked belongs to the family of *dissipatons* while anything that remains unaffected by the blockade of free energy supply belongs to that of *equilibrons*. Some examples of these two classes of structures are given in Table 15.4.

- There are many examples of *dissipatons* produced inside the cell, including the time-dependent changes in RNA levels in budding yeast measured with DNA microarrays which correlate with cell functions (Figs. 9.1, 12.2a) (Ji et al. 2009a). These so-called RNA kinetic patterns (also called “RNA trajectories”, *ribons*, or *RNA waves*; see Sect. 12.7) can be visualized on a 2-dimensional plane as shown in Figs. 12.10 and 12.11.
- One of the most distinct features of the molecular theory of the living cell being developed in this book is what is here referred to as the *Dissipaton-Cell Function Identity (DCFI) Hypothesis* which was also referred to as the *IDS-Cell Function Identity (ICFI) Hypothesis* in Sect. 12.5. This hypothesis asserts that *dissipatons* and *cell functions* are the two sides of the same coin. That is, *dissipatons* and *cell functions* are the internal (or *endo*) and external (*exo*) views, respectively, of the same phenomenon known as the living cell.
- If we designate intracellular *dissipatons* associated with some cell function as  $X$ , the following generalization holds, because the activity (or level) of  $X$  must be able to undergo either an increase or a decrease whenever the cell needs in order to adapt to changing environment. Therefore, there must exist two processes, one producing  $X$  and the other destroying it as depicted in Fig. 15.2.
- All cell functions can be accounted for, at least in principle, in terms of  $X$ , a set of molecules (e.g., enzymes, ATP, ions, RNA, etc.) whose kinetic patterns (also called behaviors, trajectories, or dissipatons) “cause” or “are correlated with” cell functions. This is the content of the *DCFI hypothesis* mentioned in 3 above.
- Finally, it is suggested here that Fig. 15.2 can be applied to what goes on in the *extracellular space* (ECS), if we assume that there exists  $X'$  in ECS which is both produced (from  $X$  as a part of  $F$ ) and destroyed in a manner similar to  $X$  in Fig. 15.2 so as to maintain its kinetic patterns to produce all extracellular structures and processes needed for all cell functions including morphogenesis. We will refer to this idea as the *Dissipative Structure Theory of Morphogenesis* (DSTM). Figure 15.4 schematically depicts the elements of DSTM.

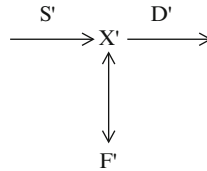


**Fig. 15.4** An *external* (or *exo*) view of the “dissipative structure theory of morphogenesis” (DSTM).  $S'$  = synthesis of  $X'$  in extracellular space (ECS).  $D'$  = destruction of  $X'$  in ECS.  $F'$  = Extracellular functions, including the construction and destruction of extracellular matrix, the production and control of pericellular ion, metabolite, and intercellular messenger gradients.  $X'$  includes extracellular matrix proteins, and  $S'$  includes exocytosis of precursor proteins of  $X'$ , and  $D'$  includes the various matrix metalloproteinases. In contrast, Fig. 15.2 can be viewed as an *internal* (or *endo*) view of the “dissipative structure theory of morphogenesis”

## 15.6 The Tree-Ring-and-Landscape (TRAL) Model of Evolutionary and Developmental (EvoDevo) Biology

*Dendrochronology*, the science of tree-ring dating, uses tree rings as a means to determine not only the age of trees but also to reconstruct the climate changes, since climate affects the tree growth and tree rings thus serve as a historical record of climate changes. The American astronomer A. E. Douglass (1867–1962) originally developed this technique in the first half of the twentieth century in order to understand cycles of sunspot activity. He reasoned that changes in solar activity would influence climate patterns on the earth which would in turn affect tree-ring growth patterns. In other words, Douglass correctly inferred the sequence of events shown in Fig. 15.5.

The main purpose of dendrochronology as developed by Douglass was to infer the sunspot activities from the tree-ring growth patterns. The purpose of morphogenetic research in biology is to understand how DNA and environmental changes bring about the shape changes in organisms within their lifetimes, that is, to understand the molecular mechanisms by which DNA and environment interact to bring about morphogenesis (Fig. 15.6).

Figures 15.5 and 15.6 have more common features than may appear on the surface. First, the tree ring is a relatively simple example of morphology. Second, sunspot activities and the associated climate changes constitute a part of the environment of organisms. Third, although not explicitly indicated in Fig. 15.5, tree rings are affected not only by sunspot activities and associated climate changes but also by the genome (i.e., DNA) of trees because different species of trees produce different tree-ring patterns even under identical environmental conditions. Therefore, Fig. 15.6 is a more comprehensive representation of the causal relations underlying morphogenesis and hence subsumes Fig. 15.5 and *dendrochronology*.

It is interesting to note that the causal scheme shown in Fig. 15.6 can be applied to either *developmental biology* or *evolutionary biology*, depending on the timescales adopted. On the time scale of individual organism’s life span



**Fig. 15.5** Tree rings can record sunspot activities, because sunspot activities affect climate which in turn influences tree-ring growth

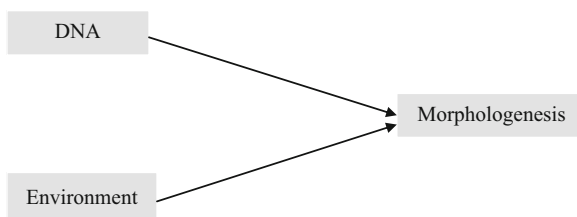


**Fig. 15.6** DNA and environment as independent cause of the morphology of organisms. The main question in morphogenesis is: What are the mechanisms by which the combination of DNA and environment brings about the morphology of organisms. Please note that environment includes sunspot activities

(i.e., in synchronic time; see Table 15.3), Fig. 15.6 represents developmental biology; on the time scale of species life span which may be as long as hundreds or more life span of the individual members of a species under consideration (i.e., diachronic time scale), the same figure can represent evolutionary biology. Thus, it may be necessary to recognize two kinds of timescales in biology – developmental (or synchronic) and evolutionary (or diachronic) times – and these timescales may be said to be *complementary* to each other in the sense that focusing on one automatically excludes the other from view just as focusing on the wave nature of light (or forest) automatically excludes the particle nature of light (or trees) from view in physics and *vice versa*.

We may express this situation as in Statement 15.6:

The biological time is complementary union of developmental (or synchronic) time and evolutionary (or diachronic) time. (15.6)

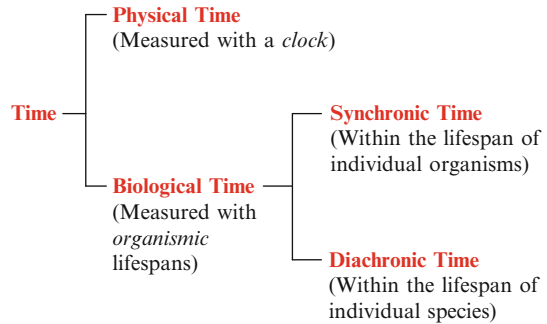
Statement 15.6 may also be referred to as the *EvoDevo duality of life* in analogy to the *wave/particle duality* of light in physics.

Both developmental and evolutionary processes can be represented using the language of *renormalizable networks* discussed in Sect. 2.4. The network characteristics of development and evolution are summarized in Table 15.5.

Of course, different species have different life spans, which can range from 1 day to  $10^6$  days. So what distinguish synchronic from diachronic timescales are not the absolute lengths of time measured with a clock as done in physics but rather the number of replication cycles of organisms which is unique to biology. In other words, synchronic and diachronic times are measured relative to the unit of the life span of organisms whereas the conventional time in physics is measured with a *clock*, which naturally leads to the possibility of dividing time into *physical* and *biological* times as schematized in Fig. 15.7.

**Table 15.5** The network representation of the *EvoDevo duality of life* in biology in analogy to the wave/particle duality of light in quantum physics

	Devo (development)	Evo (evolution)
1. <i>Node</i>	Fertilized egg cells	Organisms
2. <i>Edge</i>	Synchronic interactions ( <i>within the life span of an individual organism</i> )	Diachronic interactions ( <i>within the life span of a species</i> )
3. <i>Goal</i>	Mature organisms	Mature species

**Fig. 15.7** *The dual dichotomy of time.* That is, dichotomizing time into *physical* and *biological* times on the one hand and the biological time into *synchronic* and *diachronic* times on the other

The synchronic time is confined within the life span of the organisms of a species (e.g., days for bacteria and decades for *Homo sapiens*) and the diachronic time extends beyond individual life span and implicates hundreds or more of them, depending on the nature of the evolving traits under consideration.

Dichotomizing time into physical and biological times as shown in Fig. 15.7 appears reasonable in view of the fact that there are two distinct kinds of irreversible processes in nature – (1) *physical irreversible processes* such as diffusion of gases and radioactive decays of some elements, and (2) *biological irreversible processes* including cell division and cell death which have never been observed to be reversible. Any irreversible processes can be used as a *clock* to measure time. One major difference between *physical time* and *biological time* is the constancy of time interval or duration in the former (in non-relativistic frameworks) (Hawking and Mlodinow 2010) and the flexibility or variability of time interval or duration in the latter (e.g., the life span or generation time of bacteria is in hours as compared to that of humans which is in tens of years).

Just as dendrochronology as represented in Fig. 15.5 can be viewed as a subdiscipline of the EvoDevo duality of life as depicted in Fig. 15.6, the pattern of tree rings (combined with the image of landscape symbolizing the probability space) appears to provide a convenient *visual representation* of the EvoDevo duality of life as schematized in Fig. 15.8.

This so-called Tree-Ring-And-Landscape (TRAL) model of the EvoDevo duality of life can be applied to either *development* or *evolution* separately, not together, just as wave-measuring and particle-measuring apparatuses cannot be used together to study the nature of light (Bohr 1933, 1958, Herbert 1987). The TRL model, when



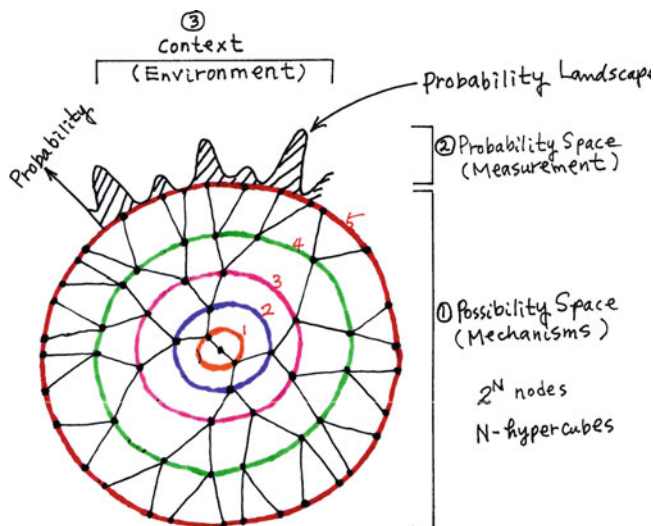


**Fig. 15.8** The “Tree-Ring-And-Landscape” (TRAL) model of the EvoDevo duality of life (in analogy to the wave/particle duality of light). Each *circle* has  $2^N$  cells, where  $N$  is the number of circles starting from the center which is assigned the value of  $N = 0$ . Each node has  $2^n$  possible internal states, where  $n =$  the number of genes in the cell

applied to *morphogenesis* (one of the three branches of developmental biology, the other two being *growth* and *differentiation*), has the following characteristics:

1. Each circle represents one *cell generation* which is exposed to an environment that may or may not change with time.
2. The number of *cells* (represented as nodes or vertices) on the  $N$ th circle is  $2^N$ , where  $N$  is the number of cell generations. When  $N = 0$ , there is one cell (at the center of the tree rings); when  $N = 1$ , there are two cells (or nodes) on the first circle; when  $N = 2$ , there are four cells on the second circle, etc.
3. The cells/nodes on any concentric circle carry a set of  $n$  genes in their DNA. The set of  $n$  genes can be represented in terms of a string of  $n$  0's and 1's, enabling the functional state of the cell to be characterized by the patterns of the distribution of 0's (inactive genes) and 1's (activated genes). The total number of possible cell states is  $2^n$ . In other words, each node on a circle has a set of  $2^n$  possible internal states (not shown) that can be represented as a string of  $n$  1's and 0's. (The  $n$  genes are renormalized as a node.)
4. Thus the TRAL model provides a convenient visual method for representing one (stem) cell growing into a system of  $2^N$  cells, each cell occupying one of the  $2^n$  cell states compatible with the prevailing environmental conditions:

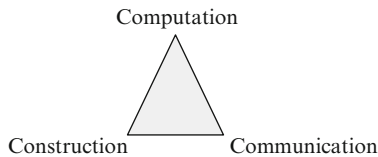
$$2^N = \text{cell number}$$

$$2^n = \text{cell states}$$

5. The  $N$ th circle (or ring) of the TRAL model can be described as an  $N$ -dimensional hypercube with  $2N$  nodes, each node having characteristics

**Table 15.6** The definition of the c-triad, assumed to be the necessary and sufficient condition for cell life including morphogenesis (Ji and Ciobanu 2003)

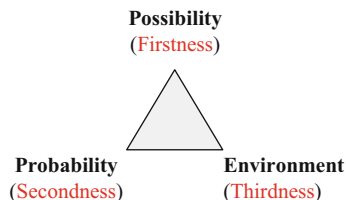
<i>C-Triad</i>	Description
1. <i>Computation</i>	Cells are evolutionarily programmed to express only those genes that promote the survival of the organisms (of which they are parts) under given environmental conditions
2. <i>Construction</i>	Cells manufacture their structural components and intercellular messengers before undergoing cell division, under the control of the environment (through synchronic interactions) and the genome (through diachronic interactions)
3. <i>Communication</i>	Cells communicate synchronically with one another by exchanging messenger molecules in order to cooperate to accomplish tasks beyond the ability of individual cells

**Fig. 15.9** A diagrammatic representation of the C-triad (Ji and Ciobanu 2003). The three processes are postulated to be both necessary and sufficient to account for the molecular mechanisms underlying the life of the cell

describable in terms of an  $n$ -bit string of 1's and 0'. Thus, the circles of the TRAL model and hypercubes are mathematically equivalent or isomorphic. All the cells (i.e., nodes), except the original cell at the center, are connected by three links each forming a Y in the centrifugal direction (i.e., from the center toward the periphery), reflecting the fact that one cell gives rise to two cells with the precursor cell disappearing as the result of cell division.

6. Within any time period (e.g., an average cell cycle time), only one ring, that is, the outermost ring, is present or realized with all the associated precursor rings having disappeared into the past (unlike the real tree rings which accumulate).
7. The outermost ring is associated with a probability space erected perpendicular to it to encode the probabilities of observing particular gene-activity states of the cells on the ring determined by the current cellular environment, the gene-activity states being represented by strings of  $2n$  1's (a gene turned on) or 0's (a gene turned off).
8. The gene-activity state of a cell, in combination with the cell environment, is thought to determine the three fundamental activities of the cell, that is, computation, construction, and communication (see Table 15.6 and Fig. 15.9).
9. Therefore, the shape or topology of the probability landscape (to be referred to as the probability distribution function of cell states [PDFCS]) erected on the outermost ring (which resembles the topology of a landscape) is determined by both the current gene-activity states of the cells (which in turn determine

**Fig. 15.10** The approximate correspondence between the triadicty of the TRAL model of life (Fig. 15.8) and the triadic metaphysics of C. S. Peirce (1903) (Sect. 6.2.2)



the activities of the C-triad) and their environmental conditions and carries all the information that can be observed/measured about an organism consisting of  $2N$  cells, each cell endowed with  $n$  genes, that are organized in space and time, including its morphology. Thus defined, PDFCS described by the TRAL model is akin to the wave function in quantum mechanics (Herbert 1987, Morrison 1990).

10. The principle of dendrochronology is this: As the cells divide, the diameter of the tree increases with time. Due to the dependence of the rate of cell divisions on the temperature and other factors of the environment of the tree, the density of cells in the tree varies with the seasons of the year – the highest density being found every winter. So the ring structure of a tree results from the interactions between two processes – the cell division (which is internal to the tree) and the rotation of the Earth around the Sun (which is external to the tree). This principle of dendrochronology may be generalized and extended to morphogenesis, since a similar, although much more complex, process can account for the structures visible on the cross section of the *Drosophila* embryos which are the results of the interaction between the internal cell division/differentiation and the external alterations of environment (including temperature, humidity, morphogen gradients, etc.). Just as we can now read off the age (and the past environmental conditions) of a tree from tree rings, so we should in principle be able to read off the developmental and evolutionary history (or mechanisms) of *Drosophila melanogaster* from the molecular and cellular architectonics of the *Drosophila*.

One unexpected result of the TRAL model is that it provides a clear visual distinction between “possibility” and “probability”. Possibility is Firstness of Peirce, probability is Secondness, and Environment is Thirdness by default (Sect. 6.2.2) (Fig. 15.10):

## 15.7 Quorum Sensing in Bacteria and Cell–Cell Communication Networks

Quorum sensing refers to the phenomenon exhibited by a group of bacteria that expresses select sets of genes *if and only if* there are a sufficiently large number of them around (hence “quorum”) to cooperatively accomplish a gene-encoded task that cannot be accomplished by individual bacteria (Miller and Bassler 2001).

This phenomenon was discovered by two independent groups about 40 years ago (Fuqua and Greenberg 2002). The seemingly intelligent behavior of bacteria is the natural consequence of the following networks of structures and processes that interact with one another in an organized manner:

1. Bacteria possess the genes coding for diffusible intercellular messengers called *autoinducers*.
2. Bacteria possess the genes coding for the cell membrane receptors recognizing and importing the autoinducers present in the pericellular space.
3. Bacteria possess the genes that code for signal transducing proteins that, when activated by extracellular autoinducers binding to their target receptors, are able to search for and express the set of genes encoding the proteins that can implement quorum-sensitive or quorum-dependent effector functions.

An example of a bionetwork embodying these elements organized in space and time so as to exhibit quorum sensing is given in Fig. 15.11, which consists of nine nodes and seven edges. The network representation in this figure is a simple and convenient way of keeping track of all the main components and their interactions involved in effectuating quorum sensing. This bionetwork is best viewed as an example of *dissipative structures* at resting state and, when the system is activated to exhibit the phenomenon of quorum sensing, the system can be said to undergo a state transition from the resting to the activated states. Figure 15.11 is not an equilibrium structure because most of the structures shown in this figure would disappear upon cessation of free energy supply to the cell. An activated state of dissipative structures is characterized by a selective activation of a subset of the nodes of the bionetwork involved, leading to space- and time-organized physicochemical processes that appear to us observers as *quorum sensing*. The extracellular or cell–cell communication components of quorum sensing can be viewed as “intercellular dissipative structure” and represented as a bionetwork wherein cells themselves serve as nodes and molecule-mediated interactions among them as edges. Hence quorum sensing can be viewed as a *bionetwork of bionetworks*, reminiscent of the “renormalization” phenomenon in bionetworks discussed in Sect. 2.4. Thus the notion of bionetwork is one of those concepts in biology that can be applied to multiple levels *recursively* and hence may be at least partially responsible for the phenomena of *self-similarity* and *power laws* universally found in living systems (Gribbin 2004, Whitfield 2006).

It is surprising to find how simple the set of molecular structures and processes are that can give rise to the seemingly intelligent behaviors of bacterial quorum sensing. Quorum sensing in bacteria may be regarded as one of the simplest cases of *cellular intelligence* and *cellular computing*, and we can now confidently say that we have a more or less complete understanding of the molecular mechanisms underlying one of the simplest intelligent behaviors of organisms. That is, there is no mystery about *cellular intelligence*. It simply is yet another example of *self-organizing chemical reaction–diffusion processes* or *dissipative structures of Prigogine*. Hence, we may logically refer to the intelligent behaviors of cells as the X-ator following the naming tradition established in the field of self-organization (Babloyantz 1986), X indicating the name of the city most closely associated with the pioneering

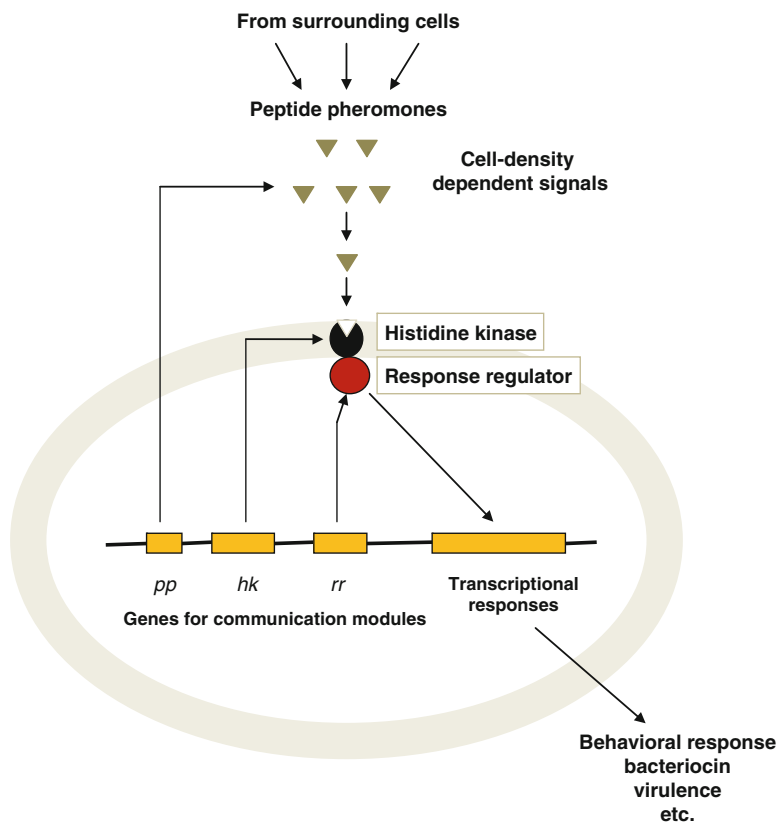


**Fig. 15.11** Mechanisms underlying *quorum sensing* in bacteria. Quorum-sensing bacteria carry four classes of genes (see the four *dark bars* along the DNA symbolized by the horizontal line) coding for (1) pheromones (also called *autoinducers*, symbolized by *triangles*), i.e., small signal molecules secreted into the extracellular medium, (2) receptor (see the *dark sphere*) for recognizing pheromones (mainly from other bacteria) and having histidine kinase activity, (3) response regulator (see the *white sphere*) required to transduce the extracellular signal, and (4) genes required for behavioral responses such as production of bacteriocins (proteins that kill certain strains of bacteria), biofilm formation (for group protection), and virulence (ability to overwhelm host's immune system response) (Adopted from the figure published at <http://www.sibelle.info/oped31.htm>)

research on quorum sensing. To the best of my knowledge, Princeton is a good candidate for X, but unfortunately, the name Princeton has already been used to label the self-organizing reaction–diffusion system responsible for the origin of biological information proposed by P. Anderson and his coworkers at Princeton University in the early 1980s, namely, the Princetonator (Ji 1991a, pp. 224–225) (see Fig. 13.3). To get out of this dilemma, it is suggested here that a city nearby Princeton be *commandeered* to serve as Princeton's surrogate. Trenton may be the logical choice for this purpose, since Trenton is the capital city of the State of New Jersey where Princeton University is located. Hence, we may refer to any self-organizing

chemical reaction–diffusion system capable of exhibiting intelligent behaviors such as quorum sensing in bacteria as the *Trentonator*. Thus, quorum sensing in bacteria is the first *Trentonator* to be characterized in molecular terms. I would not be surprised if human intelligence will turn out to be the result of a set of elementary *Trentonators* that are spatiotemporally organized within our brains, nor if there exists a minimum number of neurons ( $10^2$ – $10^3$  ?) that is needed to form the basic *Trentonator* responsible for human intelligence.

## 15.8 Morphogenesis as a Form of Quorum Sensing

Morphogenesis or shape development is a multicellular phenomenon. Therefore, there is the distinct possibility that cells will cooperate in morphogenesis just as they do in quorum sensing. *Drosophila melanogaster* is the best studied model organism for morphogenesis. *Drosophila* morphogenesis starts with a fertilized single-celled egg which becomes a multicellular embryo with structured tissues and specialized cells and organs. This process occurs through many cell divisions, shape changes, and cell migrations called gastrulation. What is interesting about morphogenesis from a theoretical point of view is this: The initially symmetrical embryo undergoes a series of *symmetry breaking processes* to become a less symmetric structure. In other words, the *Drosophila* embryo undergoes state transitions from *disordered* to *ordered* states, to use the terminology of condensed matter physics of critical phenomena (Landau and Lifshitz 1990). Thus, *symmetry breakings* and *disorder–order transitions* may be regarded as two of the most fundamental processes in morphogenesis. The first mathematical model of symmetry breaking in morphogenesis was proposed by A. Turing in 1952 (Gribbin 2004) which is based on three elementary processes – (1) A catalyzes the formation of A and B, (2) B inhibits the formation of A, and (3) A and B have different diffusion constants. These three elements were necessary and sufficient to produce *symmetry breakings* in chemical concentration fields (Gribbin 2004, p. 127).

The simplest symmetry-breaking process in *Drosophila* morphogenesis involves what is known as “convergent extension,” in which cells in a two-layer configuration migrate vertically so as to form one-layered cells with an increased horizontal length. Such cellular rearrangements are well within the capability of cells, since they are self-organizing chemical reaction diffusion systems endowed with the ability to execute the c-triad, i.e., *communication*, *computation*, and *construction* (see Table 15.6) (Ji and Ciobanu 2003). Consequently, *Drosophila* cells in this stage of development can (1) communicate with one another by synthesizing and secreting one or more morphogens (akin to autoinducers in bacteria) which diffuse away from the cells that produce them, (2) can compute the number of neighboring cells based on the combined concentrations of the morphogens secreted by neighboring cells, and (3) when the morphogen concentrations exceed a threshold value, can trigger the signal transduction cascade, leading to turning on or off of a set of genes needed to rearrange cells to produce the right embryological structure, for example, *convergent extension*. These same processes are involved in the phenomenon of quorum sensing in bacteria presented in Sect. 15.7.

Another fundamental feature of embryogenesis is that, throughout its process, there occur micro–meso correlations, because morphogenesis is ultimately directed by the molecular sequence information encoded in DNA which is located in the nucleus of individual cells. If this interpretation is right, it may be concluded that embryos are physical systems at critical points at the micro-, meso-, and macrolevels. In a sense, embryogenesis is a critical phenomenon, which may be referred to as a *bio-critical* phenomenon in contrast to the purely physical ones studied in condensed matter physics (Anderson 1972, Fisher 1998, Domb 1996).

## 15.9 Carcinogenesis as Quorum Sensing Gone Awry

Normal cells show the phenomenon of *contact inhibition*: that is, normal cells stop dividing when they make contact with adjacent cells. In contrast, cancer cells lose this ability and continue dividing in the presence of neighboring cells, thereby leading to piling up of cells on top of one another, a characteristic feature of tumor.

There appears to be the possibility that the same mechanism used by bacteria in their quorum sensing activity may be involved in normal-to-cancer cell transformation. This idea is explained in Table 15.7.

The key assumption underlying Table 15.7 is that the mechanisms of intercellular communication/cooperation observed in bacteria also operate in principle in normal density-sensitive cell growth which requires cell–cell communication through gap junctions (Evans and Martin 2002, Trosko 2007). When this cell–cell communication is compromised (dynamically as compared to statically, as explained below), carcinogenesis and angiogenesis may occur (Trosko 2007, Luiza et al. 2007). It is assumed here that what passes through gap junctions between adjacent cells is not just equilibrium structures (e.g., ions, ATP, etc.) but *dissipative structures* (or *dissipatons*), namely, the time-dependent patterns of changes in the concentrations of equilibrium structures comparable to what is referred to as RNA dissipatons (the patterns of distribution of RNA trajectories) in Sect. 12.8.2 (see also Sect. 3.2). If this idea turns out to be correct, one might predict that it is not the differences in gap junctional structures alone that

**Table 15.7** The hypothesis that carcinogenesis is a form of quorum sensing gone awry

	Quorum sensing	Carcinogenesis
1. Signal	Autoinducers	Transcription signals (less than 1,000 Da)
2. Receptor	luxR	Gap junctions (connexons)
3. Gene expression induced by	High levels of autoinducers detected by luxR	High levels of transcription signals accumulating in cancer cells due to gap junction blockade
4. Intercellular communication	Enhanced	Inhibited
5. Dissipative structures	Concentration gradient of autoinducers	Concentration gradient of transcription signals (e.g., ions, ATP, NADH, etc.?)

characterize normal vs. cancer cells but the dynamic patterns (e.g., fluctuating levels of ions maintained as the balance between the input through the gap junctions on one part of a given cell and the output through the gap junctions on another part of the same cell) that differentiates the intercellular messages being exchanged between normal cells, between normal and cancer cells, and between cancer cells.

## 15.10 Symmetry Breakings in Morphogenesis and Cosmogenesis

There may be an interesting analogy between the Big Bang theory in cosmology and the developmental biology including morphogenesis. In both cases, relatively homogeneous (i.e., symmetric or disordered) (Landau and Lifshitz 1990) initial states are transformed into heterogeneous (i.e., asymmetric or ordered) states as a function of time (see Figs. 15.1 and 15.12 and Table 15.8). In other words, in both

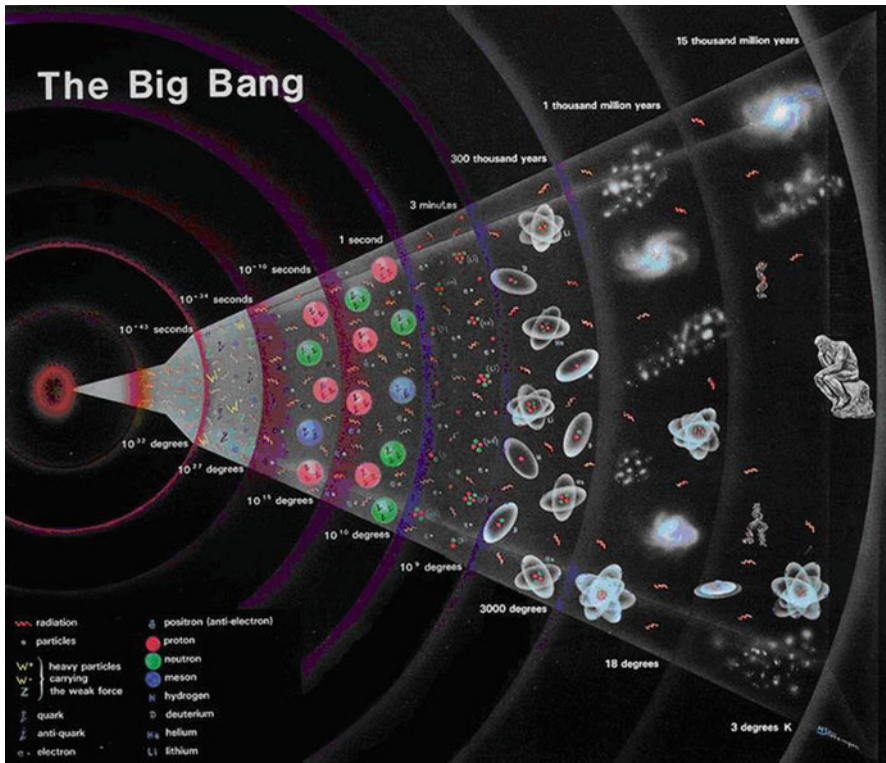


**Fig. 15.12** The evolution (or morphogenesis) of the Universe. The initially *homogenous* (symmetric) mixture of electrons, quarks, gluons, and other particles becomes heterogeneous with time. The *geometric symmetry* (or homogeneity) of the Universe is continuously broken from the *left* to the *right*. After about 13.7 billion years, the Universe contains a *heterogeneous* (symmetry-broken) mixture of galaxies, stars, planets, and other objects (Reproduced from J. Gillies 2007)



**Table 15.8** The history of symmetry breakings in the Universe

Concentric circles in Fig. 15.8	Time since time after the Big Bang	Temperature (degrees)	“Mattergy” (Sect. 2.3.1)
1	$10^{-43}$ s	$10^{32}$	Radiation (i.e., energy), matter, antimatter
2	$10^{-34}$ s	$10^{27}$	Radiation, matter, antimatter, quarks, gluons, W- and Z-particles
3	$10^{-10}$ s	$10^{15}$	Radiation, matter, antimatter, quarks, anti-quarks, electrons, positrons
4	$10^{-5}$ s	$10^{10}$	Radiation, electrons, positrons, protons, neutrons, mesons
5	3 min	$10^9$	Radiation, electrons, H, D, He, Li
6	$3 \times 10^5$ years	$6 \times 10^3$	Radiation, H and other atoms
7	$10^9$ years	18	Radiation, atoms, galaxies
8	$15 \times 10^9$ years	3	Radiation, stars, planets, DNA, <i>Homo sapiens</i>

cases, the algorithmic complexity of the systems involved (defined as the number of bits in the shortest string of symbols needed to describe an object or situation; see Sect. 4.3) increases, ultimately is driven by the increase in universal thermodynamic entropy (Sect. 2.1.4). This is why it seems logical to state that both the Big Bang and biological development (and biological evolution as well) can be viewed as examples of symmetry-breaking processes in space and time.

The cosmological symmetry breaking is generally known to be caused by the lowering of the temperature secondary to cosmological expansion (thus reducing the kinetic energy or momenta, i.e., velocity x mass, of particles) (see Fig. 15.12 and Table 15.8). However, biological symmetry breakings occur at constant temperatures (e.g., all the morphological changes shown in Fig. 15.1 occur within a narrow range of physiological temperatures), thus without slowing down thermal fluctuations or the Brownian motions of molecules and ions. Thus, we may associate *cosmogenesis* with “non-isothermal” or “cooling-driven” symmetry breakings (which will decrease *kinetic* energies of particles) and *morphogenesis* with “isothermal” or “constant temperature” symmetry breakings. In morphogenesis what is reduced may be construed to be the average distance between cognate binding surfaces of particles (including ions, molecules, biopolymers, and cells), thereby affecting their *potential* energies. Just as *momenta* (i.e., kinetic energies) and *positions* (affecting potential energies) are *complementary conjugates* in physics (Table 2.9), it may be that the *cosmological evolution* and *biological evolution* are also fundamentally related. There may be two (and only two) basic mechanisms of symmetry breakings in the Universe.

1. The “kinetic” mechanism where increased order results from reduced *kinetic energy* of binding partners, and
2. The “position” mechanism where increased order is caused by the reduction in the average distances between cognate particles (accompanied by decreased *potential energies*) in two ways – (a) via “passive” Brownian motions of binding partners and (b) via “active” translocation of binding partners driven by free energy dissipation.

We may refer to (2a) above as the “passive symmetry-breaking” mechanism, and (2b) as the “active symmetry breaking” mechanism. The cosmological (excluding biological) symmetry breakings may belong to the category of *passive symmetry breakings*, but living systems may utilize both *passive* and *active symmetry breakings*. These terms are related to the active and passive complexities discussed in Sect. 5.2.3.

An example of “active symmetry breakings” in morphogenesis is provided by the cell migration leading to germband expansion (Zallen 2006, Zallen and Wieschaus 2004) and an example of “passive symmetry breakings” is given by rosette formation among non-migrating cells in the germband of *Drosophila* (Zallen 2006). It seems possible that passively broken symmetry can be reversed, if some active mechanisms can intervene. This would mean that normal morphogenetic processes can implicate many active and passive symmetry-breaking processes organized in space and time, driven by free energy dissipation under the control of genetic information encoded in proteins, DNA, and RNA.

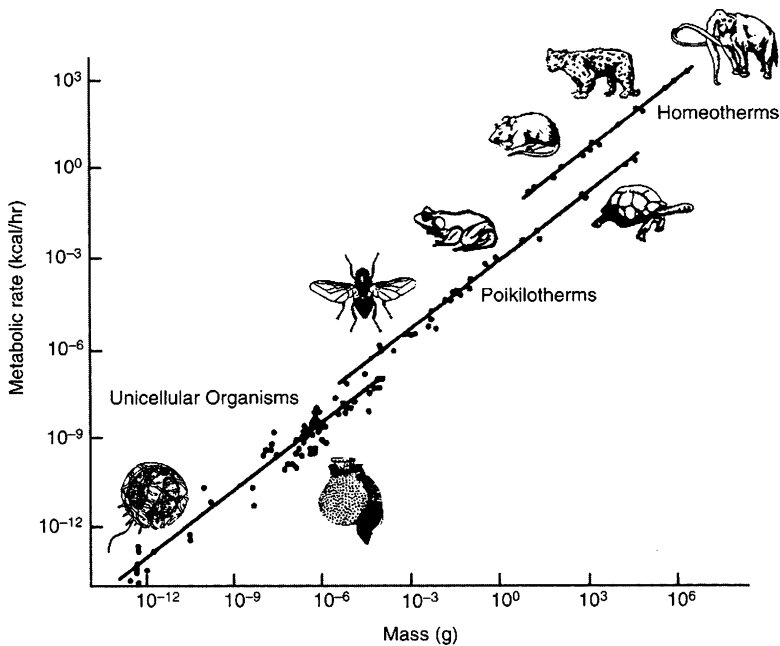
The cosmological symmetry breakings shown in Fig. 15.12 may have their counterparts in *biological symmetry breakings* exemplified by the development of a multicellular organism from a single fertilized egg cell. Biological symmetry breakings can be represented diagrammatically as bifurcation trees such as the inverted tree (Fig. 7.8) or the TRAL model (Fig. 15.8). If there are  $n$  cells in an adult organism, it will take  $(\log n / \log 2)$  generations of cell divisions for a fertilized egg cell to become an adult organism. Since there are about  $10^{13}$  cells in the adult human body, it will take about 40 generations ( $10^{13} \sim 2^{40}$ ) of cell divisions for a fertilized egg (see the node labeled 1 in Fig. 7.7 or the center node in Fig. 15.8) to mature into an adult human being with all its complexities. Figure 7.7, when rotated by  $90^\circ$  anticlockwise, resembles Fig. 15.12 in that the complexity (or order) of the system increases from left to right. If this comparison is valid, the Universe at the time of the Big Bang would be akin to a fertilized egg perhaps with superstrings acting as a “cosmological DNA” (Ji 1991).

Figure 7.7 was used to represent the postulate that enzymes can be viewed as coincident (event) detectors (Sect. 7.2.2). This notion can be better illustrated if Fig. 7.7 is rotated  $90^\circ$  clockwise. In this orientation, the leaves at the fifth level of branching (i.e., the nodes labeled 16–31) can be thought to represent Brownian particles or thermally fluctuating physicochemical processes, and the nodes at the next level (i.e., the nodes labeled 8–15) represent coincidence-detecting events. The leaves in Fig. 7.7 can be thought of as molecular events (e.g., enzymic reactions) which affect the next higher level (e.g., gene expression) which in turn affect the next higher level (e.g., cell divisions) and so on until the root (e.g., an embryo) is reached. Interpreted in this manner, Fig. 7.7 can be viewed as the mechanism for coupling genotype and phenotype, or microscale events and macroscale events, without any thermal gradients and hence as a system of dissipative symmetry breakings. In other words, these nodes are events (requiring  $x$ ,  $y$ ,  $z$ , and  $t$  to be specified and hence 4-dimensional in nature) that occurs if and only if two or more lower-level events occur more or less synchronously, that is, within a certain time window or bin,  $\Delta t$ , with intensities equal to or greater than the threshold,  $\Theta$  (see Eq. 7.18 in Sect. 7.2.2). The root of the bifurcation tree, namely, node 1, is a

dynamic system whose structure and function are driven by a system of such coincident events, and we can identify such a system with an organism, unicellular or multicellular. Viewed in this manner, cells and their higher-order systems whose structure and properties ultimately depend on enzymes can be naturally associated with a 4-dimensional space. In other words, living systems are 4-dimensional and can be projected onto either the traditional 3-dimensional space of Euclid at a given time (span) or the one-dimensional space of time under a given spatial arrangement.

## 15.11 Allometry

Allometry is the study of the effect of the size of an organism, either unicellular or multicellular, on its function. For example, the linear relation between metabolic rates and body mass of different organisms shown in Fig. 15.13 is the subject of intense studies in the field of allometry. Whitfield defines *allometry* as follows (2006, p. 58):



**Fig. 15.13** The relationship between the metabolic rate of various organisms and their body mass (Reproduced from Whitfield 2006, p. 77 with kind permission from Novo Nordisk, Inc.)

The relationship between metabolic rate and body weight is an example of a biological pattern called allometry, which compares how the value of any biological trait, such as metabolic rate or leg length, changes with the total size of a plant or animal. (15.7)

The so-called *quarter-power scaling laws* (Whitfield 2006, pp. 78–79) stating that many biological traits scale as body mass raised to the power of one or more quarters may be derived from the postulate that *the phenomenon of life is 4-dimensional because enzymes are coincidence detectors* (see Sect. 7.2.2). The *allometry equation* has the following deceptively simple form:

$$y = ax^b \quad (15.8)$$

where  $y$  is biological trait, either processes or structures,  $x$  is the total size of a cell, a plant or animal, and  $a$  is the *allometric coefficient*, and  $b$  is the *allometric exponent* which can be greater or less than 1. If  $b$  is greater than 1, for example, as in the case of deer antlers, the trait gets proportionately larger, and, if  $b$  is less than 1 as is the case with metabolic rate, it gets proportionately smaller so that, when the body size doubles, the metabolic rate increases by less than twofold.

During the past one and a half century, it has been found that, over a very wide range of body sizes of organisms (covering 27 orders of magnitude from unicellular organisms to whales), the metabolic rate scales as (or is proportional to) the body mass raised to the power of approximately  $3/4$  (White and Seymour 2005). In Fig. 15.13, the metabolic rates of organisms from single cells to the elephant are plotted against their body masses on a log–log scale. The figure has three parallel lines, one each for *homeotherms*, *poikilotherms* (also called ectotherms), and *unicellular organisms*. They all have the same slope, that is,  $b = 3/4$  but intercept the  $y$ -axis at different points, resulting in different values for  $a$ : The lower the intercept, the lower the *average* metabolic rate for each group. The allometric exponent of shown in this figure is not the only possibility. There are many cases where it differs from and hovers around  $2/3$  (see Table 1 in White and Seymour 2005). It will be assumed here that the power law reflects at least some of the principles underlying the scaling phenomena in biology and that even the allometric exponent of  $2/3$  may be viewed as an example of the quarter-power scaling since  $2/3$  is equal to  $2.666/4$ . Thus, any viable theory of allometric scaling should be able to provide a reasonable theoretical basis to account for the numerical values of both  $a$  and  $b$  in Eq. 15.8. It should be noted here that certain traits such as life span, heart beats, blood circulation time, and unicellular genome length scale as the body mass raised to the power of  $1/4$ , and the radii of aortas and tree trunks scale as body mass raised to the power of  $3/8$  or  $1.5/4$  (West and Brown 2004). These are examples of “quarter-power scaling,” and the key question that has been challenging theoretical biologists for more than a century is why these exponents are multiples of  $1/4$ , not  $1/3$  as expected on the basis of the scaling in the Euclidean space.

One of the currently most widely discussed and intensely debated theories to account for the  $3/4$  allometric exponent of the power law relating metabolic rate ( $y$ ) to body mass ( $x$ ) is the one proposed by West and Brown (2004, Whitfield 2006). Their theory accounts for the  $3/4$ th scale exponent on the basis of the assumption that

natural selection evolved hierarchical fractal-like branching networks that distribute energy, metabolites, and information from macroscopic reservoirs to microscopic sites. (West and Brown 2004) (15.9)

They further postulated that the hierarchical branching networks provided the following constraints:

1. Networks service all local biologically active regions in both mature and growing biological systems. Such networks are called space filling.
2. The networks' terminal units are invariant within a class or taxon.
3. Organisms evolve toward an optimal state in which the energy required for resource distribution is minimized.

It is interesting to note that the concept of networks employed by West and his coworkers (e.g., animal circulatory systems, plant vascular systems) focuses on the static spatial and geometric aspect of bionetworks, which may be viewed as belonging to the class of the *equilibrium structures* of Prigogine (Sect. 3.1.5). Since living systems are dynamic and better described in terms of *dissipative structures* (Prigogine 1977, 1980, Ji 1985a, b), and since living processes are almost always mediated by enzymes whose behaviors can be best characterized in terms of "temporal networks" in contrast to "spatial networks" as pointed out in Sect. 7.2.3, it may be reasonable to formulate an alternative theory of allometric scaling based on the notion of *dissipative network*, which are at least 4-dimensional in the sense that it takes four coordinates to characterize them, namely,  $x$ ,  $y$ ,  $x$ , and  $t$ .

Therefore, a simple explanation for the quarter-power scaling laws may be derived on the basis of the following assumptions:

1. The body mass ( $x$ ) of an organism is not a geometric object (i.e., *equilibrium structure*) but a 4-dimensional entity, because it can be viewed as an organized system of cells and processes catalyzed by enzymes (acting as coincidence detectors) (see Fig. 7.8 in Sect. 7.2.3).
2. The number of cells ( $n$ ) of an organism can be viewed as the projection of organisms on to the 3-dimensional Euclidean space (i.e., devoid of the time dimension).
3. The metabolic rate ( $y$ ) of an organism is directly proportional to the number of cells constituting that organism (whose Euclidean volume is  $v$ ), the proportionality constant increasing with both body temperature ( $T$ ) and cell density,  $d = n/v$ , defined as the number of cells per unit body volume. (For simplicity, it will be assumed that the mitochondrial contents, or better the average respiratory activities, of cells are invariant among individual organisms and across species.)

Based on Assumptions (1) and (2), we can write:

$$n \sim x^{3/4} \Rightarrow n = ax^{3/4} \quad (15.10)$$

Based on Assumption (3), we can write:

$$y \sim n \quad (15.11)$$

Combining Eqs. (15.10) and (15.11) leads to:

$$y_i = a_i x_i^{3/4} \quad (15.12)$$

where  $y_i$ ,  $a_i$ , and  $x_i$  are, respectively, the metabolic rate, the proportionality constant and the body size of the  $i$ th species with a distinct cell density,  $d_i$ , and habitat temperature,  $T_i$ . Because of Assumption (3),  $a_i$  is a function of both  $T_i$  and  $d_i$ :

$$a_i = f(d_i, T_i) \quad (15.13)$$

Taking the logarithm of both sides of Eq. (15.12) leads to:

$$\log y_i = \frac{3}{4} \log x_i + \log a_i \quad (15.14)$$

Equation (15.14) predicts that, when the  $i$ th metabolic rate,  $y_i$ , is plotted against the  $i$ th body mass,  $x_i$ , on a double logarithmic coordinate system, a straight line with slope  $3/4$  would be obtained with different  $y$ -intercepts for different species, consistent with Fig. 15.13. Designating unicellular organisms as 1, poikilotherms as 2, and homeotherms as 3, the data in Fig. 15.13 make it clear that  $a_1 < a_2 < a_3$ , indicating that the metabolic rates per unit mass increase from unicellular organisms to poikilotherms to homeotherms. This observation is consistent with the *FERFAC* (Free energy requirement for Active complexity) hypothesis, Statement 15.20, which predicts that organisms with higher active complexities require higher energy expenditures, since the *active complexity* (Sect. 5.2.3) of the groups of the organisms considered here most likely increases in the same order as their intercept values,  $a_i$ .

The life span (LS) of an organism can be viewed as the projection of the living processes embodied in  $x$  on to the time dimension, which leads to:

$$LS_i = a_i x^{1/4} \quad (15.15)$$

where  $LS_i$  and  $a_i$  are, respectively, the life span and the proportionality constant of the  $i$ th species. Equation (15.15) is qualitatively consistent with the life span vs. body-mass plots found in the literature (e.g., see <http://www.senescence.info/comparative.html>) and (West and Brown 2004).

The key difference between the West–Brown–Enquist (WME) approach to developing a theory of allometric scaling and the one proposed in this book is that the former assumes that the  $3/4$  exponent can be derived mathematically from the species-specific physical characteristics of organisms (e.g., vascular trees of mammals, diffusion paths within cells in unicellular organisms), whereas the present approach regards the exponent as resulting from the universal property of all living systems, i.e., enzymic activity, regardless of differences in distribution networks among different individuals and species. It is possible that both approaches are relevant, since living systems embody two distinct processes – *transport* of matter between micro-meso (e.g., cells) and macro-sites (e.g., lung) and *transformation* of matter within cells. Based on the structural information of all living systems (e.g., role of mitochondrial membranes and lung alveoli membranes), it is likely that transport processes scale as the body mass raised to the power of  $2/3$  as was first suggested by Rubner in 1883 (White and Seymour 2005), and, based on the idea that

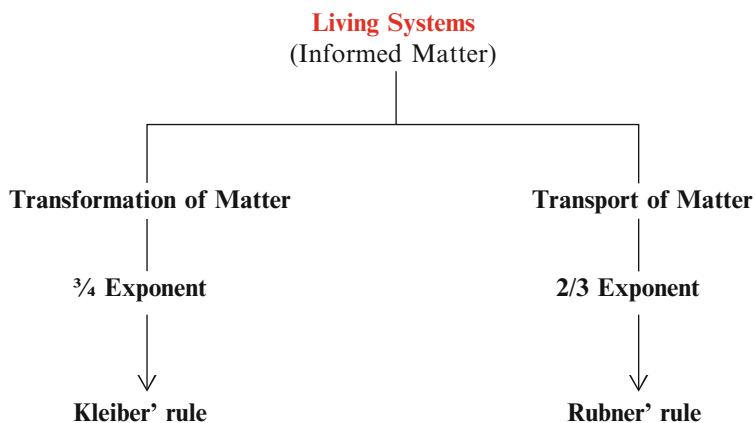


**Fig. 15.14** The living systems as *informed matter* defined as the complementary union of matter/energy and information/life (see Table 2.5 in Sect. 2.3.1) that is supported by two dichotomous processes – *mass transformation* and *mass transport*, ultimately driven by chemical reactions catalyzed by enzymes acting as coincidence detectors (see Sect. 7.2.2)

enzymes are coincidence detectors serving as the nodes of temporal branching networks (Fig. 7.7), it can be suggested that transformation of matter in cells scale as the body mass raised to the power of  $3/4$ , as proposed above. It is also possible that certain dynamic traits are rate-limited by *transport* of matter and that of certain others by *transformation* of matter, depending on the evolutionary, ontogenic, and physiological conditions of the organisms under consideration, thereby exhibiting either the  $2/3$  or  $3/4$  allometric exponents or some values in between as seems to be the case (see Tables 1 and 2 in White and Seymour 2005). These ideas are summarized in Fig. 15.14.

As evident in Fig. 15.15, the level of non-protein-coding DNA (i.e., dr-genes defined in Sect. 11.2.4) relative to protein-coding DNA (drp-genes, Sect. 11.2.4) is found to increase rapidly with increasing biological complexity, for example, from unicellular to multicellular organisms. The ratio of noncoding DNA to the total DNA does not change much from *Nanoarchaeum equitans* through *Rickettsia conorii* (spanning 67 unicellular species) but begins to rise sharply with *Rickettsia prowazekii*, continuing to rise through 19 species (multicellular species), reaching the maximum ratio with *Homo sapiens* (Mattick 2004). One plausible interpretation of the data in Fig. 15.15 is that the noncoding portions of DNA encode the information needed to organize in space and time the cells in multicellular organisms in order to maintain their functions. This idea can be expressed using the language of network sciences (Sect. 2.4) (Barabasi 2002, 2009):

The coding regions of the DNA of a multicellular organism determine the intrinsic properties of the nodes of a bionetwork and the noncoding DNA regions determine both the interactions among the nodes and the space- and time-dependent control of their interactions in order to accomplish evolutionarily selected functions of the organism. (15.16)

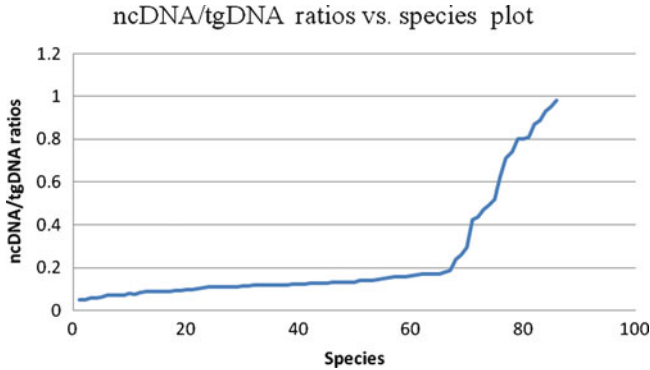


**Fig. 15.15** The ratio of non-protein-coding (dr-genes, Sect. 11.2.4) to protein-coding DNA (drp-genes) in various species. The ratio does not change much from *Nanoarchaeum equitans* through *Rickettsia conorii* (spanning 67 species) but begins to rise sharply with *Rickettsia prowazekii*, continuing to rise through 19 species, reaching the maximum ratio of 0.983 with *Homo sapiens*. The data were downloaded from Taft and Mattiack 2012. ncDNA = noncoding DNA; tgDNA = total genomic DNA. The ncDNA/tgDNA ratio values were obtained from (Taft and Mattiack, arXiv.org/ftp/q-bio/papers/0401/0401020.pdf, downloaded on 01/04/2012; see also Mattiack 2004). The coordinate values of the organisms plotted on the x-axis are: 1 = *Nanoarchaeum equitans*, 2 = *Thermotoga maritima*, 3 = *Campylobacter jejuni*, 4 = *Wolinella succinogenes*, 5 = *Borrelia burgdorferi*, 6 = *Auifex aeolicus*, 7 = *Helicobacter hepaticus*, 8 = *Ureaplasma urealyticum*, 9 = *Treponoma pallidum*, 10 = *Archaeoglobus fulgidus*, 11 = *M. thermoautotrophicum*, 12 = *Mycoplasma pulmonis*, 13 = *Pyrococcus horikoshii*, 14 = *Mycobacterium tuberculosis*, 15 = *Mycobacterium bovis*, 16 = *Helicobacter pylori* 26695, 17 = *Dienococcus radiodurans*, 18 = *Helicobacter pylori* J99, 19 = *Caulobacter crescentus*, 20 = *Listeria monocytogenes*, 21 = *Listeria innocua*, 22 = *Fusobacterium nucleatum*, 23 = *Pseudomonas aeruginosa* PAO1, 24 = *Aeropyrum pernix*, 25 = *Coxiella burnetii*, 26 = *Chromobacterium violaceum*, 27 = *Pasteurella multocida*, 28 = *Streptomyces coelicolor*, 29 = *Chlorobium tepidum* TLS, 30 = *Prochlorococcus marinus*, 31 = *Agrobacterium tumefaciens*, 32 = *Mycoplasma genitalium*, 33 = *Pyrobaculum aerophilum*, 34 = *Prochlorococcus* MED4, 35 = *Clostridium acetobutylicum*, 36 = *Enterococcus faecalis*, 37 = *Xyella fastidiosa*, 38 = *Eschelichia coli* 0157:H7, 39 = *Eschelichia coli* K-12, 40 = *S. enterica* serovar Typhi CT18, 41 = *Vibrio cholera*. 42 = *L. lactis* sp. *Lactis* IL1403, 43 = *Ralstonia solanacearum*, 44 = *Streptococcus* MGAS315, 45 = *Thermoanaerobacter tengcongensis*, 46 = *Thermoplasma acidophilum*, 47 = *Brucella melitensis*, 48 = *Bacillus subtilis*, 49 = *P. syringae* pv. *Tomato* DC300, 50 = *Buchnera aphidicola* (Ap), 51 = *Methanococcus jannaschii*, 52 = *Mesorhizobium loti*, 53 = *Yersinia pestis*, 54 = *Xanthomonas axonopodis*, 55 = *Haemophilus influenzae* Rd, 56 = *Bacillus halodurans*, 57 = *Xanthomonas campestris*, 58 = *Bacillus anthracis*, 59 = *Bacillus cereus*, 60 = *Buchnera aphidicola* (Bp), 61 = *Staphylococcus aureus* N315, 62 = *Staphylococcus aureus* Mu50, 63 = *Clostridium perfringens*, 64 = *Buchnera aphidicola* (Sg), 65 = *Nisseria meningitides*, 66 = *Prochlorococcus* MIT9313, 67 = *Rickettsia conorii*, 68 = *Rickettsia prowazekii*, 69 = *Encephalitozoon cuniculi*, 70 = *Saccharomyces cerevisiae*, 71 = *Schizosaccharomyces pombe*, 72 = *Dictyostelium discoideum*, 73 = *Plasmodium falciparum*, 74 = *Plasmodium yoelii* yoelii, 75 = *Typanosoma brucei*, 76 = *Neurospora crassa*, 77 = *Arabidopsis thaliana*, 78 = *Caenorhabditis elegans*, 79 = *Oryza sativa* L. ssp. *japonica*, 80 = *Oryza sativa* L. ssp. *indica*, 81 = *Drosophila melanogaster*, 82 = *Ciona intestinalis*, 83 = *Fugu rubripes*, 84 = *Anopheles gambiae*, 85 = *Mus musculus*, and 86 = *Homo sapiens*



In Sect. 2.4.1, a bionetwork was defined as a network of nodes ( $\mathbf{n}$ ), such as proteins, RNA, and DNA, connected by edges ( $\mathbf{e}$ ) according to some topology ( $\mathbf{T}$ ) so as to accomplish a biological function ( $\mathbf{F}$ ), that is,  $\mathbf{F} = \mathbf{T}(\mathbf{n}, \mathbf{e})$ . Statement 15.16 satisfies all the requirements of the definition of a bionetwork with the following identifications:

1.  $\mathbf{F}$  = “evolutionarily selected functions of the organism”
2.  $\mathbf{T}$  = “the noncoding DNA regions determine ...the space- and time-dependent control of their interactions...”
3.  $\mathbf{n}$  = “...coding regions of the DNA ...determine the intrinsic properties of the nodes ...”
4.  $\mathbf{e}$  = “the noncoding DNA regions determine ... the interactions among the nodes”

Therefore, based on the empirical data shown in Fig. 15.15 and the bionetwork theory described in Sect. 2.4.1, it is possible to make the following equivalent or related generalizations:

DNA of an organism encodes a bionetwork. (15.17)

DNA is a molecular representation of a bionetwork. (15.18)

Since DNA is a molecular representation of a bionetwork and since a bionetwork is a graph-theoretical representation of an organism, DNA is a molecular representation of an organism. (15.19)

Statement 15.19 may be referred to as the *Bionetwork Theory of DNA* (BTD), and it is here suggested that BTD complements the Watson-Crick theory of DNA (Watson and Crick 1953) which is mostly *structural* (or *node-centered*, in the language of network sciences).

At least 50% of the non-protein-coding DNA of the human genome has been found to code for RNA molecules that are not translated into proteins (Mattick 2004). Hence, Fig. 15.15 indicates that the level of RNA in cells most likely increases with biological complexity, making RNA levels inside the cell (and associated non-protein-coding DNA, or dr-genes; Sect. 11.2.4) a reliable index of the complexity (the active kind; see Sect. 5.2.4) of the phenotype of multicellular organism. Since maintaining complex structures of organisms would entail free energy dissipation, the following generalization follows:

The more complex an organism is, the more energy *the organism needs* to survive. (15.20)

We will refer to Statement 15.20 as the *Hypothesis of the Free Energy Requirement for Active Complexity of Living Systems* or more briefly as the *Free Energy Requirement for Active Complexity* (FERFAC) (for the definition of “active complexity”, see Sect. 5.2.3). As discussed in connection with Fig. 15.13, the allometric data on the log–log relation between the body weight vs. the metabolic rate of various species, i.e., Eq. (15.14), strongly support the validity of the *FERFAC* hypothesis.

## 15.12 Micro–Macro Coupling in the Human Body

The human body is arguably the most complex material system in the Universe (besides the Universe Itself) in both its *structure* and *behavior*. The human body consists of approximately  $10^2$  joints,  $10^3$  muscles,  $10^3$  cell types, and  $10^{14}$  neurons, each with multiple connections to other neurons (Kelso 1995). In addition, the motions of these components are not random but *coordinated* so that the body can perform macroscopic tasks essential for its survival under prevailing environmental conditions. The purpose of this section is to apply the theoretical principles and concepts developed in this book to elucidating the possible mechanisms underlying the phenomenon of the micro–macro coupling we experience in *coordinated motions* of our body.

*Coordination dynamics* originated in the study of the *coordination* and *regulation* of the movements of the human body (Bernstein 1967, Kelso 1995, Kelso and Zanone 2002, Kelso and Engström 2006, Kelso 2008, 2009) but its principles are *scale-free*, i.e., *scale-independent*, and *universal* in that they apply to all material systems at all levels, including microscopic and macroscopic levels, that have more than one components interacting with one another to accomplish observable functions, leading to the following definition:

Coordination dynamics is the study of the space-, time- and task-dependent interactions among the components of a dynamic system. (15.21)

We may recognize three broad branches of coordination dynamics on the basis of the distance scale over which coordination processes take place:

1. *Macroscopic Coordination Dynamics* (MacroCD) = the study of coordinated motions of the components of a system at the macroscopic scale (e.g., coordinated motions of left and right limbs, coordinated motions among the fingers of a hand),
2. *Mesoscopic Coordination Dynamics* (MesoCD) = the study of coordinated motions of the components of a system at the mesoscopic scale (e.g., morphogenesis; see Sect. 15.1), and
3. *Microscopic Coordination Dynamics* (MicroCD) = the study of coordinated motions of the components of a system at the molecular level (e.g., coordinated motions of the ATP-binding and  $\text{Ca}^{++}$ -binding domains of the  $\text{Ca}^{++}$  ion pump; see Figs. 8.6 and 8.7).

The human body movement depends on the successful coordination of all the components of the body on these three distance scales. The physicochemical systems embodying coordination dynamics at the three scales are distinct as schematically shown in Fig. 15.16. The theoretical concepts (*conformons*, *IDSs*, and *synergies*) that have been invoked as the mechanisms enabling the coordination dynamics at the three distance scales are indicated in Fig. 15.16, along with the suggested names of the associated dynamical systems (*RMWator*, *Bhopalator*, and *BocaRatonator*). *RMWator* and *BocaRatonator* are the two names used here for the first time, and the rationale for coining them is given in the legend to Fig. 15.16 and in Footnotes 24

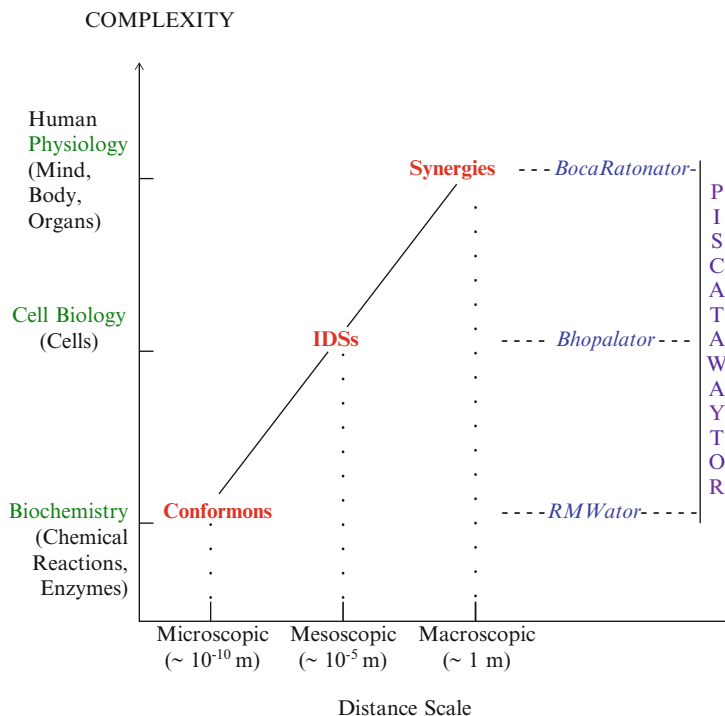


**Fig. 15.16** Conformons, IDSs (Intracellular Dissipative Structures) (Sect. 3.1.2), and synergies as *microscopic*, *mesoscopic*, and *macroscopic* manifestations of *gnergons* (Sect. 2.3.2) or *dissipatons* (Sect. 3.1.2). The *gnergon*-based model of human behavior is here referred to as the “BocaRatonator” to acknowledge the seminal contributions made by Kelso and his colleagues at the Florida Atlantic University at Boca Raton, Florida. The term “RMWator” derives from **R** (Richland, to acknowledge Xie and his colleagues for their measurement of single-molecule enzymic activity of cholesterol oxidase while at The Pacific Northwest National Laboratory in Richland, WA), **M** (Minneapolis, to acknowledge Rufus Lumry and his colleagues’ fundamental contributions to enzymology at the University of Minnesota at Minneapolis), and **W** (Waltham, to acknowledge the seminal work on enzyme catalysis carried out by William Jencks and his group at the Brandeis University in Waltham, Mass)

and 26 to Table 15.10. The theoretical model of the human body as a whole that is based on the *principle of self-organization* was referred to as *the Piscatawaytor* in (Ji 1991) (see Fig. 15.18). The various *ators* appearing in Fig. 15.16 are related as shown in Eq. (15.22) where CD stands for coordination dynamics:

$$\text{Piscatawaytor} = \frac{\text{RMWator}}{(\text{MicroCD})} + \frac{\text{Bhopalator}}{(\text{MesoCD})} + \frac{\text{BocaRatonator}}{(\text{MacroCD})} \quad (15.22)$$

In December 2008, Professor Kelso visited Rutgers for 3 days and gave informative and inspiring seminars on *coordination dynamics* and the philosophy of *complementary pairs* to both my General Honors Seminar students and a

**Table 15.9** The similarities and differences between the biological theories developed by J. A. S. Kelso and S. Ji

	Kelso (1984, 2008)	Ji (1974a, b, 2000, 2004a)
1. System studied	Human body	Molecular machines
2. Methods	Cognitive neuroscience Nonlinear dynamics	Chemistry Molecular mechanisms
3. Principles invoked	Synergies Biological information Self-organization Complementarity	Gnergons <sup>a</sup> Biological information Self-organization Complementarity
4. Direction of generalization	Macro → micro	Micro → macro
5. Philosophical generalization	Complementary nature (Kelso and Engström 2006)	Complementarism (Ji 1993, 1995)

<sup>a</sup>Gnergons are discrete units of gnergy, the complementary union of *energy* and *information* (Sect. 2.3.2). Gnergons are thought to be necessary and sufficient for all self-organizing, goal-directed motions in all physical systems including the cell and the human body. Examples of gnergons include conformons (Chap. 8) and IDSs (Chap. 9)

University-wide audience. During his visit at Rutgers, we had an opportunity to compare the results of our researches over the past several decades in our respective fields of specialization and it did not take too long for us to realize that we have been studying the same forest called the human body albeit from two opposite ends – Kelso and his coworkers from the *macroscopic end* of human body movements and I from the *microscopic end* of molecular and cell biology. The similarities and differences between these two approaches and the results obtained are summarized in Table 15.9. Evidently, between us, we have covered the whole spectrum of *the science of the human body*, from *molecules to mind* (as Kelso poetically put it over breakfast one morning). One way to visualize how Kelso’s poetic vision might be realized in material terms is shown in Fig. 15.17, the essence of which can be stated as follows:

Mind controls cells; cells control molecules; molecules control energy supply and thereby cells and mind. (15.23)

Statement 15.23 reminds us of the *reciprocal causality* or *cyclic causality* where A affects B which then affects A back, etc. (Kelso and Engström 2006, pp. 115,191). We may refer to Statement 15.23 as the “Reciprocal Causality of Mind and Molecules” (RCMM). It may be significant that the source of *control information* and that of *free energy* are located at the two opposite ends of the diagram, reflecting the fact that control information originates in the mind and the energy needed to implement the control instruction can come only from the chemical reactions catalyzed by enzymes.

Table 15.10 characterizes the three branches of coordination dynamics operating within the human body in detail and situates the works of Kelso and mine within the triadic framework of coordination dynamics. As Row 1 indicates, the human body can be viewed as an excellent example of a *renormalizable bionetwork* discussed in Sect. 2.4. That is, the human body is a network of cells, each of which is a network

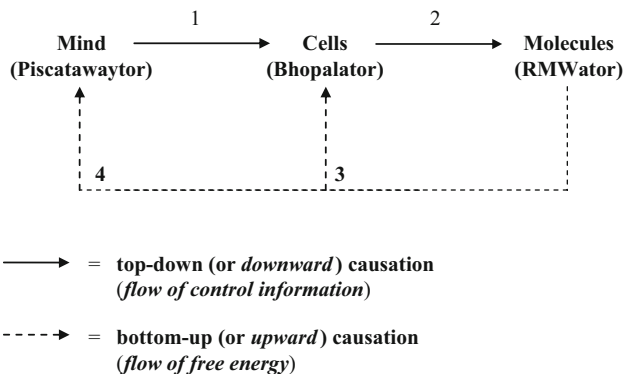


**Fig. 15.17** The *Principle of the Reciprocal Causality of Mind and Molecules (RCMM)* mediated by cells, or more briefly the *Principle of Mind-Molecule Coupling (PMMC)*. Step 1 represents the action of mind on cells, as when I decide to lift a cup by activating neurons in my motor cortex which in turn activate the muscle cells in my arm and fingers. Step 2 represents the action potential–triggered activation of the myosin ATPase molecules in muscle cells that catalyze the hydrolysis of ATP, the source of free energy. The free energy released from ATP hydrolysis in muscles and the brain powers all the motions in muscle cells (Step 3) and neurons in the body which constitute the mind (or the brain) (Step 4). It will be shown in Footnote 26 below that this figure embodies what is referred to as the *First Law of Coordination Dynamics (FLCD)*. Mind (viewed as a part of the human body), cells, and enzyme molecules in action are examples of dissipative structures (or *dissipatons*) and hence can be named as X-ators, where X is the name of the city where the most important research is done on a particular “ator.” The acronym RMW stands for Richland, Minneapolis, and Waltham (see Footnote 27 in Table 15.10)

**Table 15.10** Coordination dynamics at three distance scales

		Coordination dynamics at three scales		
		Macroscopic (~1 m)	Mesoscopic (~10 <sup>-5</sup> m)	Microscopic (~10 <sup>-10</sup> m)
1. Renormalizable bionetwork <sup>a</sup>	Node	Cells	Biopolymers	Atoms
	Edge	Intercellular messenger- mediated cell–cell interactions <sup>b</sup>	Noncovalent interactions <sup>c</sup>	Covalent interactions <sup>d</sup>
2. Experimental data	Bio-network	Human body	Cells	Biopolymers
	Kelso	e.g., lip and jaw movement in speech production		
	Ji	(a) Human anatomy <sup>e</sup>  (b) Pain pathways <sup>f</sup> (c) Brain reward system <sup>f</sup>	(a) Metabolic Pathways <sup>g</sup>  (b) Genome-wide microarray data <sup>h</sup>	(a) DNA supercoils <sup>i</sup>  (b) Single- molecule enzymology <sup>j</sup>
3. Methods	Kelso	(a) Biomechanical <sup>k</sup> (b) Nonlinear dynamical <sup>l</sup>		

(continued)

**Table 15.10** (continued)

		Coordination dynamics at three scales		
		Macroscopic (~1 m)	Mesoscopic (~10 <sup>-5</sup> m)	Microscopic (~10 <sup>-10</sup> m)
	Ji	(a) Anatomical <sup>c</sup>	(a) Molecular biological <sup>n</sup>	(a) Physical <sup>p</sup>
		(b) Physiological <sup>c</sup>	(b) Cell biological <sup>o</sup>	(b) Chemical <sup>q</sup>
		(c) Pharmacological <sup>m</sup>		(c) Single-molecule
	enzymological <sup>f</sup>			
4. Key concepts	Kelso	Synergies <sup>s</sup>	(synergies) <sup>t</sup>	(synergies) <sup>t</sup>
	Ji	Renormalizable bionetworks <sup>a</sup> (dissipatons, SOWAN machines, or gnergons) <sup>u</sup>	IDSs <sup>u</sup> (dissipatons, SOWAN machines, or gnergons) <sup>u</sup>	Conformons <sup>v</sup> (dissipatons, SOWAN machines, or gnergons) <sup>u</sup>
5. Models based on PSO <sup>w</sup>	Kelso	BocaRatonator <sup>x</sup>		
	Ji	Piscatawaytor <sup>y</sup>	Bhopalator <sup>z</sup>	RMWator <sup>aa</sup>

of biopolymers, and biopolymers are networks of atoms. It is interesting to note that each bionetwork is characterized by a unique mechanism of interactions among its nodes – short-range *covalent interactions* among atoms to form biopolymers; medium-range *noncovalent interactions* among biopolymers to form cells; and long-range *messenger-mediated interactions* among cells to form the human body. Extensive footnotes are attached to most of the items appearing in Table 15.10, often with their own tables and figures (reminiscent of nested networks of self-similarity).

<sup>a</sup>Biological networks where a node can become a new network at a higher resolution and a network can become a node of another network at a lower resolution (see Sect. 2.4). For example, at the microscopic level, atoms (e.g., H, O, C, N, deoxyribonucleotides) are the nodes of a network known as a biopolymer (e.g., DNA); at the mesoscopic scale, biopolymers are the nodes of a network known as the cell; and at the macroscopic scale, cells constitute the nodes of a networks known as the human body.

<sup>b</sup>This type of interactions make it possible for long-distance interactions or communications between cells, over distances ranging from 0 (e.g., contact inhibition) to meters (e.g., hormone-mediated or axon-mediated connections).

<sup>c</sup>Relatively weak and ATP-independent interactions or bonds requiring only about 5 kcal/mol to break.

<sup>d</sup>Relatively strong, enzyme-catalyzed, interactions or bonds requiring 50–100 kcal/mol to break (Moore 1963, p. 57).

<sup>e</sup>According to the triadic definition of function (Sect. 6.2.11), *structures* (including anatomy; see Figs. 15.19 and 15.20) are as important as *processes* (including physiology) and *mechanisms* to account for functions.

<sup>f</sup>Much is known about the neuroanatomy and neurophysiology underlying the effects of pain and pleasure on human body motions.

<sup>g</sup>Metabolic pathways encoded in a cellular genome are akin to the keys on a piano keyboard (*equilibrons*) and metabolic activities observed in living cells are comparable to the melodies (*dissipatons*) that a pianist produces by striking a select set of keys obeying the instructions given in a sheet music.

<sup>h</sup>The DNA microarray technology allows us to measure (hear) the dynamic changes (audio music) in RNA levels (or waves) occurring within a living cell in response to environmental perturbations. Microarrays make it possible to visualize the coordinated interactions among select RNA molecules in a living cell under a given environmental condition (see Figs. 12.1 and 12.2).

<sup>i</sup>Visual evidence for the concept of conformons (see Sect. 8.3).

<sup>j</sup>Dynamic evidence for the concept of conformons (see Sect. 11.4.1).

<sup>k</sup>For example, the continuous monitoring of the thumb movement in both hands (Kelso 1984).

<sup>l</sup>According to Kelso and Engstrøm (2006, pp. 90–91),

Coordination dynamics, the science of coordination, is a set of context-dependent laws or rules that describe, explain, and predict how patterns of coordination form, adapt, persist, and change in natural systems. . . . Coordination dynamics aims to characterize the nature of the functional coupling in all of the following: (1) within a part of a system, as in the firing of cells in the heart or neurons in a part of the brain; (2) between different parts of the same system, such as between different organs of the body like the kidney and the liver, or between different parts of the same organ, like between the cortex and the cerebellum in the brain, or between audience members clapping at a performance; and (3) between different kinds of things, as in organism ~ environment, predator ~ prey, perception ~ action, etc. . . . (15.24)

Coordination dynamics at the macroscopic level can be studied using the powerful tools and concepts provided by the mathematics of *nonlinear dynamics* (van Gelder and Port 1995, Scott 2005). A *coordination law* that has been found useful in analyzing real-life biological systems can be expressed as in Eq. (15.25) (Kelso and Engstrøm 2006, pp. 156–157):

$$d(cv)/dt = f(cv, cp, fl) \quad (15.25)$$

where  $d(cv)/dt$  is the rate of change of the *coordination variable*  $cv$  whose numerical value changes with the state of the system under investigation,  $cp$  is one or more *coordination parameters* that can affect the state of the system but are not affected by it, and  $fl$  is the noisy or thermal fluctuations experienced by the system.

It should be pointed out that a given mathematical idea or principle such as Eq. (15.25) can be represented in many equivalent ways. Some examples are shown below:

$$dx/dt = f(x, P, fl) \quad (15.26)$$

where  $x = cv$ , and  $P = cp$  in Eq. (15.25), or

$$dx/dt = f(cv, cp, fl), \text{ or} \quad (15.27)$$

“(rate of change in  $x$ ) is a function of  $x$ , control parameter  $cp$  and fluctuation  $fl$ ”, or most abstractly (15.28)

$$(\underline{\quad})' = f(\underline{\quad}, \underline{\quad}, \underline{\quad}) \quad (15.29)$$

where  $(\underline{\quad})'$  indicates a time derivative of whatever is inside the parenthesis,  $f$  is a mathematical function, and the underlines represent “place holders” which can be filled with appropriate variables, numbers, or words. That is, although Eqs. 15.25–15.29 all look different, their meaning is the same, and this is because mathematics employs *signs* and signs are arbitrary (see Sect. 6.1.1).

Equation (15.25) can be integrated with respect to time  $t$ , resulting in:

$$cv = F(t, cp, IC, fl) \quad (15.30)$$

where  $F$  is a new function different from  $f$ ,  $t$  is time, and  $IC$  is the integration constant whose numerical value is determined by initial conditions. According to Eq. (15.30), the so-called trajectories (see 1 below) in  $t$ - $cv$  plots depend on *initial conditions*.

Some of the basic concepts and principles embodied in the coordination law, Eq. (15.25), can be visualized using the skateboarder as an analogy. The skateboarder moving up and down the walls of the empty swimming pool is a convenient metaphor to illustrate a set of important concepts in nonlinear dynamics:

1. *Coordination variable, cv*: The position of the skateboarder on the  $x$ -axis which varies with time, increasing (movement from left to right) or decreasing (movement from right to left) as the skateboarder moves up and down the pool surface acted upon by gravity. The plot of  $cv$  against time,  $t$ , is known as *trajectories*. The shapes of the trajectories differ (i.e., the trajectories evolve in time in different ways) depending on *initial condition* (i.e., the numerical value of  $cv$  at  $t = 0$ ) and the *control parameter*  $cp$ , which is in the present case the curvature of the pool surface.
2. *Stable fixed point* also called *attractor*: The skateboarder always returns to the bottom of the pool to minimize its gravitational potential energy.
3. *Unstable fixed point* also called *repeller*: The skateboarder resting on the top of the hill is *unstable* because he/she can be easily pushed off the peak position. If the skateboarder is unperturbed (e.g., by randomly fluctuating directions of wind), he/she can remain at the precarious position forever.
4. *Potential landscape* often designated as the  $cv$ - $V$  plot: The relation between the gravitational potential energy of skateboarder's body,  $V$ , and its position on the  $x$ -axis which fixes its  $z$ -axis due to the constraint imposed by the pool surface.



5. *Control parameter* designated as cp: The *curvature* of the wall of the pool, depending on which the skateboarder moves up and down with different speeds
6. *Bifurcation*: One becoming two. For example, the trajectory of the skateboarder at the top of the hill divides into two (if he/she is pushed off) – either toward the right or the left.

<sup>m</sup>The study of the effects of drugs on human bodily motions provides insights into the mechanisms underlying human movement under normal conditions.

<sup>n</sup>Molecular interactions inside the cell are determined not only by *free energy* changes but also by the *evolutionary information* (Sect. 4.9) (Lockless and Ranganathan 1999) encoded in the structures of interacting partners.

<sup>o</sup>The cell is the smallest DNA-based molecular computer (Ji 1999a) and the unit of biological structure and function.

<sup>p</sup>Many physical principles including the Franck–Condon principle (Sect. 2.2), laws of thermodynamics and quantum mechanics provide guidelines for visualizing molecular interactions in the cell.

<sup>q</sup>Life is ultimately driven by chemical reactions and needs the principles of chemistry and chemical reactions to be understood at the fundamental level.

<sup>r</sup>For the first time in the history of science, it has become possible, since the mid-1990s, to observe enzymic reactions and molecular motor actions on the single-molecule level, providing new insights into the workings of biopolymers, including dynamic disorder (Row A, Table 11.10), molecular memory effects (Row C, Table 11.10), and coordinated motions between remote domains.

<sup>s</sup>Kelso (2008) defines a *synergy* as

a functional grouping of structural elements (molecules, genes, neurons, muscles, etc.) which, together with their supporting metabolic networks, are temporarily constrained to act as a single coherent unit. (15.31)

Thus defined a *synergy* is more or less synonymous with a *SOWAWN machine* (Sect. 2.4) and a *dissipation* (Sect. 3.1.5), both of which being examples of *gnergons* (Sect. 2.3.2). Hence *synergies may be considered as a member of the gnergon class*.

<sup>t</sup>Although the concept of the synergy originated in macroscopic science of human body motions (Bernstein 1967), the concept was subsequently extended to cellular and molecular levels (reviewed in Kelso 2008, 2009).

<sup>u</sup>*Intracellular dissipative structures* were first invoked in the Bhoplator model of the cell (Ji 1985a, b) as the final form of the expression of genes and generalized in the form of *dissipatons* and *SOWAWN machines* that were suggested to be applicable to other levels of biological organizations (Sects. 9.1, 10.1).

<sup>v</sup>Conformons were invoked in (Green and Ji 1972a, b) to account for the molecular mechanism underlying the coupling between respiration and phosphorylation reactions in mitochondria (Sects. 8.1, 8.7) and later generalized to formulate the concept of *gnergons* in (Ji 1991) which was postulated to apply to all levels of organization, both biotic and abiotic (Sect. 2.3.2).

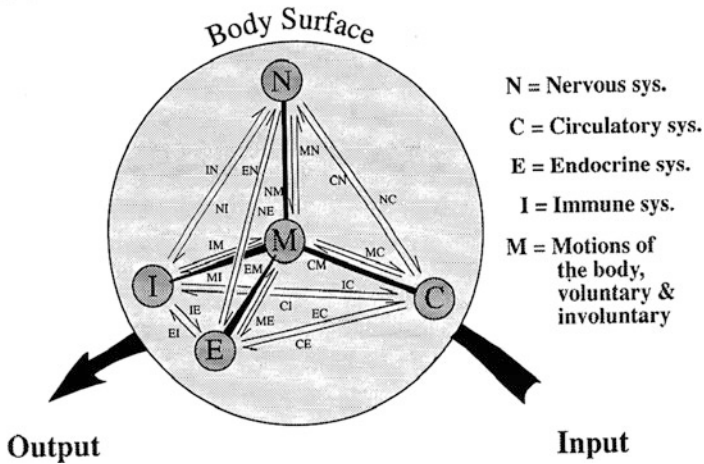


**Fig. 15.18** The Piscatawaytor. A theoretical model of the human body based on the principle of self-organization described in Sect. 3.1

<sup>w</sup>The Principle of Self-Organization (Sect. 3.1).

<sup>x</sup>The nonlinear dynamical model of the human body based on the Principle of Self-Organization. The name BocaRatonator is suggested here (as indicated earlier) to acknowledge the contributions that J.A.S. Kelso and his colleagues at the Florida Atlantic University in Boca Raton, Florida, have made in advancing the field of the coordination dynamics of the human body. The Piscatawaytor (see below), in contrast, is best considered as the theoretical model of the human body that integrates, albeit qualitatively, the molecular (micro coordination dynamics), cellular (mesocoordination dynamics), and physiological (macrocoordination dynamics) descriptions of the human body (Figs. 15.16, 15.18).

<sup>y</sup>The theoretical model of the human body comprising five basic compartments (nervous, circulatory, endocrine, immune, and motor systems) dynamically interacting with one another based on the *Principle of Self-Organization* (Ji 1991) (see Fig. 15.18).

As can be seen in Fig. 15.18, the motor system (**M**) is placed at the center of the tetrahedron, the simplex of the 3-dimensional space (Aleksandrov et al. 1984), because motion is thought to constitute the most fundamental aspect of the human body as indicated in the following quotation from Ji (1991, p. 144):

the fact that the M system must be relegated to the center of the tetrahedron in order to effectuate the simultaneous contacts suggests the possibility that the most important biological function of the human body is voluntary motions, including thought processes (emphasis added). This conclusion places voluntary motions, which we all too readily take for granted, at the center of our biological being. Is it possible that there is some deep philosophical significance to this conclusion? Have we underestimated the fundamental biological and evolutionary significance of our voluntary bodily motions? (15.32)

The idea expressed in this paragraph appears consonant with the dynamical approach to cognitive science advocated in the book entitled *Mind as Motion* edited by Port and van Gelder (1995), which motivates me to suggest that the Piscatawaytor may provide a *biologically realistic* theoretical framework for *cognitive science* of the future that can not only integrate existing paradigms (e.g., computational vs. dynamical approaches) but also open up new possibilities of research.

<sup>z</sup>The Bhopalator model of the cell at the mesoscopic level (see Fig. 2.11) may be essential in linking the microscopic and macroscopic worlds. That is,

One of the fundamental roles of the living cell in biology is to provide the mechanistic framework for coupling exergonic microscopic processes and endergonic macroscopic processes in the human body. (15.33)

Statement 15.33 is consistent with or supported by Statements 15.34 and 15.35:

It is impossible for the human body to perform macroscopic movement without driven by microscopic chemical reactions. (15.34)

The free energy that is required for all macroscopic motions of the body can only be provided by exergonic chemical reactions catalyzed by enzymes at the microscopic level. (15.35)

Statements 15.33–15.35 are also in agreement with the *reciprocal causality of the human body* depicted in Fig. 15.17, according to which the macroscopic events, that is, *mind-initiated body motions*, and the *microscopic events*, that is, *enzyme-catalyzed chemical reactions*, are coupled through the mediating role of *the living cell*. The fundamental role that the living cell plays in effectuating the bodily motions, therefore, may be more generally stated as a law:

It is impossible to couple macroscopic bodily motions, either voluntary or involuntary, and microscopic chemical reactions without being mediated by the mesoscopic living cell. (15.36)

For convenience of discussions, Statement 15.36 may be referred to as the “First Law of Coordination Dynamics” (FLCD).

There are two mechanisms of coordinating two positions or points in the human body (and in multicellular organisms):

1. The *static (rigid, equilibrium) coordination mechanism (SCM)* operating between the two ends of a bone, for example, that are connected to each other through a rigid body, and
2. The *dynamic (flexible, dissipative) coordination mechanism (DCM)* operating between two points located in the opposite ends of a muscle, a muscle fiber or in two remote domains within a biopolymer, for example, that are connected through flexible, deformable bodies.

The principles underlying SCM are provided by the *Newtonian mechanics* while those underlying DCM derive from multiple sources including the (1) *Newtonian mechanics*, (2) *thermodynamics*, (3) *quantum mechanics*, (4) *statistical mechanics*, (5) *chemical kinetics*, (6) *control theory*, and (7) *evolutionary biology* which are all implicated, although not always explicitly discussed, in what is known as

*coordination dynamics* (Bernstein 1967, Kelso 1995, Turvey and Carello 1996, Jirsa and Kelso 2004, Kelso and Enstrøm 2006).

When two objects A and B are coordinated via SCM, they are connected to a rigid body C so that A, B, and C form a mechanically coupled *simple machine* (to be called the *SCM machine*) and the movements of A and B are automatically coordinated. But when A and B are coordinated via DCM, they are connected to a deformable body C (to form what may be called the *DCM machine*) in such a manner that A, B, and C are mechanically coupled system only when appropriate conditions are met. In other words, *the DCM machine is a much more complex and sophisticated than the SCM machine. In addition, the DCM machine is synonymous with the SOAWN machine and the renormalizable network discussed in Sect. 2.4.*

The First Law of Coordination Dynamics (FLCD), Statement 15.36, is a phenomenological law similar to the laws of thermodynamics and does not provide any detailed mechanism as to how the law may be implemented in real life. To the extent that empirical data can be marshaled to formulate realistic mechanisms to implement FLCD, to that extent FLCD will gain legitimacy as a law. Figure 15.17 provides an empirically based mechanistic framework for implementing FLCD and hence can be viewed as a diagrammatic representation of FLCD. According to Fig. 15.17, FLCD consists of two causes – upward causes or mechanisms (Steps 3 and 4) and downward causes or mechanisms (Steps 1 and 2).

The *upward mechanisms* implementing FLCD implicate the hierarchical organization of material components of the muscle from the myosin molecule to the muscle attached to a bone, ranging in linear dimensions from  $10^{-10}$  to 1 m (see Fig. 15.19). Figure 15.19 exposes the essential problem underlying the upward mechanism: *How can myosin molecules move the muscle?* For example, in order for our arm to move a cup of tea or an apple, the arm muscle must generate forces in the range of 1 N acting over distances in the range of 1 m in less than 1 s (Fig. 15.19). But a myosin molecule can generate forces only in the range of 1 pN (picoNewton, or  $10^{-12}$  N) acting over distances in the range of  $10^{-8}$  m. That is,

In order for our body to move an object powered by chemical reactions, our body must (i) amplify the forces generated by individual myosin molecules from  $10^{-12}$  N to 1 N (an increase by a factor of about  $10^{12}$ ), (ii) extend the active distance of the molecular force from  $10^{-8}$  m to 1 m (an increase by a factor of about  $10^8$ ), and (iii) slow down processes from  $10^{-9}$  s to about 1 s (a factor of about  $10^9$ ). (15.37)

We may refer to Statement 15.37 as *the FDT amplification requirement* (FDTAR) for the micro–macro coupling in the human body, F, D, and T standing for *force*, *distance*, and *time*, respectively. Now the all-important question from the perspective of coordination dynamics is:

How is the FDTA requirement met in the human body? (15.38)

As a possible answer to Question 15.38, it is here suggested that there are two key principles to effectuate the FDT amplification in the human body:

1. The Chunk-and-Control (C&C) principle. This principle was discussed in Sect. 2.4.2, according to which the cell controls, for example, the replication of DNA

Size	System	Time	Force
~ 1 m	<b>Muscle</b>	~ 1 s	~ 1 N
	↑		
	<b>Fassicle</b>		
	↑		
~10 <sup>-5</sup> m	<b>Muscle Fiber</b>		
	↑		
~10 <sup>-6</sup> m	<b>Sarcomere</b>		
	↑		
	<b>Myofibril</b>		
	↑		
~10 <sup>-8</sup> m	<b>Myosin (Conformons)</b>	~10 <sup>-9</sup> s	~ 10 <sup>-12</sup> N*

**Fig. 15.19** The upward arm of the mind-molecule coupling depicted in Fig. 15.17. The macro–micro coupling in the muscle tissue by increasing the effective mass of contractile system. Myosin molecules generate mechanical energy packets known as *conformons* during the hydrolysis of ATP that myosin catalyzes (see Figure Panel d in Fig. 11.34). \*Tominaga et al. (2003)

by chunking it into six different structural units (or chunks) ranging in size from 2 to 1,400 nm in diameter (see Fig. 2.9). Similarly it is postulated here that the human body effectuates the FDT amplification by *chunking* the contractile system into six hierarchical structure ranging from (1) myosin molecules to (2) myofibrils to (3) sarcomeres to (4) muscle fibers (or muscle cell) to (5) fassicles, and to (6) skeletal muscle (Fig. 15.19).

Chunks are dissipative structures (or dissipatons) requiring continuous dissipation of free energy in order to maintain their functions. The chunks depicted in Figs. 2.9 and 15.19 are the shadows of the functional chunks of DNA and the contractile system, respectively, that are projected onto the 3-dimensional space. Cells or the human body forms their functional chunks so that they can more efficiently control the motions of DNA or the skeletal muscle, perhaps not unlike the human brain *chunking* symbols into *phonemes* (units of sound), *morphems* (units of meaning), *words* (units of denotation), *sentences* (units of judgment), *paragraphs* (units of reasoning ?), and *texts* (units of theory building?) to control the language.

2. The Principle of Synchronization (PS) through the generalized Franck–Condon mechanism (Sect. 7.2.2). The synchronization of the actions of protein domains within an enzyme is thought to be needed for effectuating catalysis (see, for example, the synchronization of the amino acid residues 1–4 at the transition state in Fig. 7.5). Synchronization is a nonrandom process and hence requires dissipation of free energy to be effectuated in order not to violate the laws of thermodynamics (see Sect. 2.1). The free energy required to synchronize amino acid residues in the catalytic cavity of an enzyme is postulated to be derived from substrate binding or the chemical reaction that the enzyme catalyzes. Organizing the catalytic residues at the enzyme active site is a relatively slow process compared to the fast electronic transitions accompanying chemical reactions that provide the needed free energy. To couple these two partial processes, the slow process must precede the fast one, according to the generalized Franck–Condon principle (GFCP) or the Principle of Slow and Fast Processes (PSFP) (Sect. 2.2). Thus, the following generalization logically follows:

Slow and fast partial processes can be coupled or synchronized if and only if i) the fast process is exergonic and ii) the slow process precedes the fast process. (15.39)

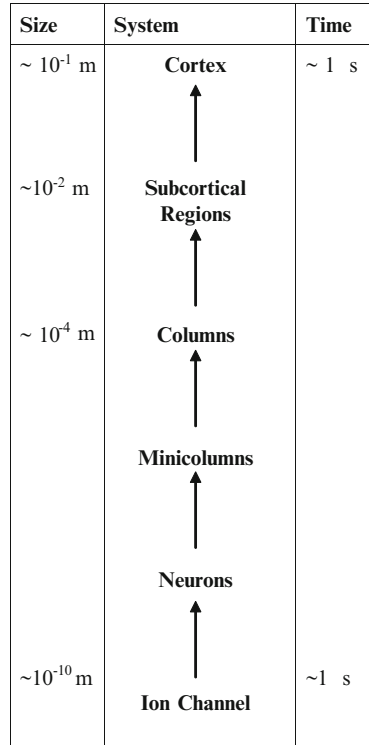
Statement 15.39 may be viewed as a more complete expression of GFCP or PSFP than the previous version given in Statement 2.25 (Ji 1991, p. 53), because it specifies the source of free energy needed to drive the coupling or the synchronization of two partial processes, one slow and the other fast: *The free energy must be supplied by the fast, not the slow, partial process.*

The synchronization phenomenon has also been observed among neuronal firing activities in the brain which is known as *neuronal synchrony* (Woelbern et al. 2002, Anderson et al. 2006, Averbeck and Lee 2004). In analogy, we may refer to the synchrony underlying enzymic catalysis (see Fig. 7.5 in Sect. 7.2.2) as the *protein domain synchrony*. Generalizing further, it is postulated here that the principle of synchrony can be extended to all *chunked systems* in biology, including the contractile system depicted in Fig. 15.19 and that, just as the *protein domain synchrony* is effectuated through the generalized Franck–Condon mechanism (GFCM) (see Fig. 7.5), so all other *chunk synchronies* depend on GFCM in order not to violate the laws of thermodynamics. The essential role of GFCM in “chunk synchrony” resides in making it possible for the synchronized system to pay for its free energy cost by coupling slow, endergonic processes to fast, exergonic process such as ATP hydrolysis or membrane depolarization triggered by action potentials. Based on these considerations, it appears reasonable to conclude that:

The dynamic actions of the chunks in chunked systems in biology and medicine can be synchronized based on the generalized Franck–Condon mechanisms or the Principle of Fast and Slow Processes. (15.40)

We will refer to Statement 15.40 as the *principle of FDT amplification by increasing mass*, or the *FDTABIM (to be read as “FDT-ah-bim”) principle*. On the level of the contractile system of the human body, the FDTABIM principle appears to be satisfied because the size of the chunks increases by a factor of about  $10^8$  from myosin to muscle and because all the chunks can be activated simultaneously by the

**Fig. 15.20** The downward arm of the *reciprocal causation of mind and molecule* depicted in Fig. 15.17. The macro–micro coupling in the brain by increasing the effective mass of computing (or decision-making) system and hence the computational power



synchronous firing of the efferent neurons of the motor cortex (see Fig. 15.20) that innervate the muscle cells. It is interesting to note that the FDTABIM principle is implemented by *nerve impulse* in the contractile system and by *thermal fluctuations* inside cells (Fig. 7.6). We will refer to the former as the “voltage-initiated” FDTABIM mechanism and the latter as the “fluctuation-initiated” FDTABIM mechanism. (Since the *chunk synchronization* is a necessary condition for FDTABIM (see (i) above), we can alternatively refer to these mechanisms as “voltage-initiated” and “fluctuation-initiated” chunk synchrony, respectively.) These two types of FDTABIM mechanisms are not independent of each other but hierarchically linked. Hence, it can be predicted that the action of the skeletal muscle, for example, will depend on both the fluctuation- and voltage-initiated FDTABIM mechanisms, although the details are not yet known.

So far we have been discussing the mechanisms underlying the transmission of force from the myosin molecules to the skeletal muscle given the synchronous activation of the muscle cells involving neuronal synchrony, namely, through the *voltage-initiated FDTABIM mechanism*. That is, we have been focusing on the *upward arm* of the *reciprocal causation* underlying the mind-molecule coupling phenomenon (see Fig. 15.17). We will now discuss the *downward arm* of the reciprocal causation of this mind-molecule coupling. The main idea here is that once the brain decides which muscle cells to activate to produce the desired bodily

motions (a *slow process*), the brain fires the right number of the right neurons in the motor cortex (a *fast process*), innervating the right set of muscle cells that then generate the needed mechanical force to be subsequently amplified through the upward causal mechanism discussed above.

The brain consists of approximately  $10^{12}$  neurons which are organized into functional cortical areas. For example, the motor cortex constitutes 6.3% of the total cortical area of the human brain or about  $100 \text{ cm}^2$  (Cook 1986, p. 69). There is experimental evidence (Cook 1986, pp. 61–73) that the neocortex is organized in terms of *column*-like structures arranged in grid-like formation, each consisting of ten to a hundred thousand neurons. The motor cortical column is about  $500 \mu\text{m}$  in diameter and contains 30,000 pyramidal cells, and there are a maximum of  $10^6$  such columns per cerebral hemisphere (Cook 1986, p. 63). Each cortical column is thought to possess a specific computational function, for example, the processing of the information from a specific whisker in a rat's mustache. Thus, the *cortical column* may be viewed as a *basic computational unit* of the cortex.

The *downward causation* of mind over molecule begins with somatic nerves that originate in the motor cortex and form the neuromuscular junctions (or end plates) on the surface of target muscle cells. Each muscle cell is innervated by one efferent somatic neuron and one such neuron can synapse with tens of thousands of muscle cells, an arrangement that seems ideal for *synchronizing* the activation of many muscle cells for the purpose of amplifying force and distance of myosin action. When activated, these nerves release the neurotransmitter, acetylcholine (Ach), at the neuromuscular junction, causing the depolarization of the postsynaptic muscle cells by opening their  $\text{Na}^{++}$  and  $\text{K}^+$  ion channels in sequence which in turn leads to the release of intracellular  $\text{Ca}^{++}$  from the sarcoplasmic reticulum. The rise in the  $\text{Ca}^{++}$  concentration in muscle cells activates a series of intracellular events, resulting in the generation of mechanical force in myosin molecules coupled to ATP hydrolysis, most likely through the conformation mechanism (see Chap. 8 and Fig. 11.34). The downward arm of the reciprocal causation of mind and molecules (Fig. 15.17) begins in the motor cortex and ends at the level of neuromuscular junction as schematically depicted in Fig. 15.20. Strictly speaking the downward causation does not implicate any molecule directly but only indirectly through depolarized cells and hence should be referred to as mind-cell coupling rather than mind-molecule coupling which should be reserved for the upward causation. In other words, *the motor neurons in the motor cortex do not communicate directly with myosin molecules but only indirectly through muscle cells which control myosin and associated molecules involved in contraction.*

As alluded to above, the downward causation also implicates coupling two partial processes – one *slow* and the other *fast*. It is here postulated that *the slow, endergonic partial process* underlying the downward causation is the thermal fluctuation-induced random and transient contact formation (or assembling) and detachment process (or disassembling) among cortical columns in the motor cortex and *the fast, exergonic partial process* is identifiable with membrane depolarization of assembled columns. *Here it is assumed that cortical columns possess structures (such as specific axon terminals) that can actively explore potential*



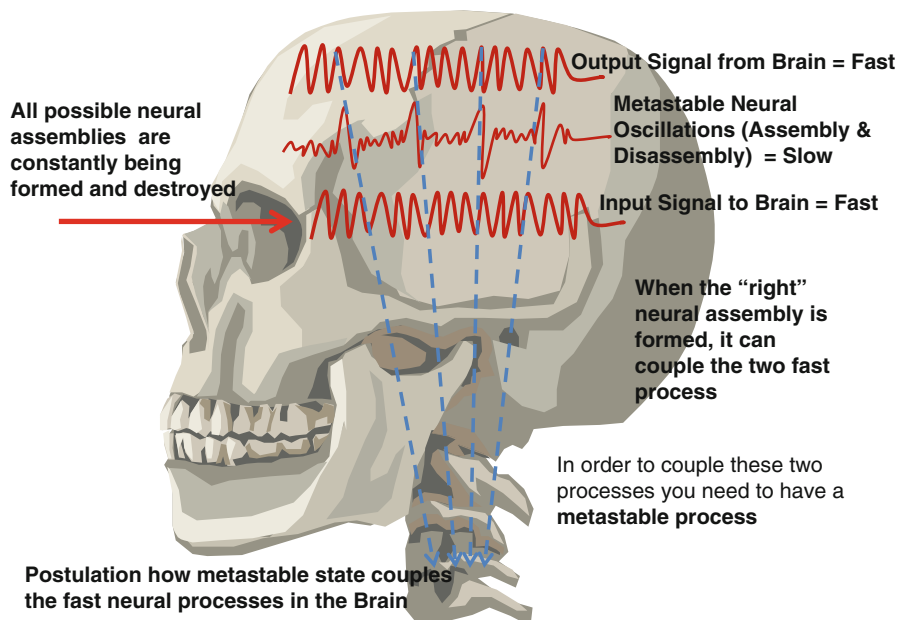


**Fig. 15.21** The generalized Franck–Condon principle postulated to underlie the coupling between (1) *the cortical column assembling/disassembling* process essential for mental activities, and (2) *synchronous firings of muscle cells* during the micro–macro coupling accompanying body motions. See text for details (*I thank Julie Bianchini for drawing this figure in December 2008*)

*postsynaptic targets in their neighborhood by undergoing random fluctuations or Brownian motions*, just as molecules undergo Brownian motions or thermal fluctuations until they find their binding sites. But the “seemingly” random motions postulated to be executed by axon terminals are active (in the sense that depolarized axon terminals are thought to be unable to undergo such explorative motions), while the random motions of molecules are passive since no free energy dissipation is involved. We will therefore refer to the seemingly random motions of axon terminals as “actively random,” “quasi-random,” or “quasi-Brownian” and the conventional Brownian motions of molecules as “passively random,” “truly random,” or just “random”. Quasi-random processes may be slower than truly random processes.

As indicated above, there are approximately  $10^6$  cortical columns in the motor cortex per hemisphere (Cook 1986, p. 63). These motor columns may undergo *quasi-random interactions*, exploring all possible patterns of interactions or configurations, and when the right configuration is selected or stabilized by input signal to the brain, that particular set of motor cortical columns is thought to be activated (or depolarized), leading to an almost simultaneous activation of their target muscle cells which results in visual input-specific body motions. This series of postulated events are schematically represented in Fig. 15.21. Using the language

of *coordination dynamics*, we may conveniently describe the transition of the motor cortex from the state where cortical columns are undergoing quasi-random explorative motions to the state where the input signal-induced depolarization of a particular configuration of cortical columns has occurred in terms of the transition from the *metastable state* to *bi-table (or multi-stable) state*. This state transition is suggested to be the result of coupling the slow column rearrangement and the fast axonal depolarization obeying the generalized Franck–Condon principle or the Principle of Slow and Fast Processes (Sect. 2.2.3).

Based on the above mechanisms, it is possible to estimate the force generated in the muscle when one cortical column in the motor cortex is activated as a result of the input of some external stimuli such as visual signals (see Fig. 15.21) through Steps 1–4 described below:

1. The activation of the efferent motor neurons constituting a cortical column in the motor cortex causes an almost simultaneous activation of the muscle cells innervated by the motor neurons.
2. The number of the muscle cells activated by one motor column is equal to  $nr$ , where  $n$  is the number of motor neurons contained in one motor column (estimated to be  $10^4$ ; see below) and  $r$  is the number of the muscle cells innervated by one motor neuron which is assumed to be  $10^3$ , leading to  $nr = 10^4 \times 10^3 = 10^7$ , the number of the muscle cells that can be activated synchronously by one column in the motor cortex.
3. We assume that the number  $m$  of the myosin molecules contained in one muscle cell is approximately  $10^4$ . Hence the number of myosin molecules activated by one motor column would be  $nrm$  or  $(10^7)(10^4) = 10^{11}$ .
4. Since one myosin molecule can generate force  $f$  in the range of  $10^{-12}$  N (see Fig. 15.21), the force generated by activating one motor column would be  $nrmf = (10^{11})(10^{-12} \text{ N}) = 10^{-1}$  N.
5. The diameter of the cortical column is  $5 \times 10^{-6}$  m and the area of the motor cortex is  $6,817 \text{ mm}^2$  (or approximately equal to a circle with  $8 \times 10^{-2}$  m in diameter) (Cook 1986, pp. 63–66). Hence the number of the columns contained in the motor cortex is approximately  $[(8 \times 10^{-2})/(5 \times 10^{-6})]^2 = [1.6 \times 10^4]^2 = 3 \times 10^8$ .
6. Therefore, the number of the motor columns that needs be activated synchronously to generate 1 N of force in the muscle to lift, say, a cup of tea or an apple (<http://en.wikipedia.org/wiki/N>) would be  $1 \text{ N}/(10^{-1} \text{ N}) = 10$ , which is small compared to the total number of cortical columns present in the motor cortex of the human brain,  $3 \times 10^8$ .

The force (F), distance (D), and time (T) amplification by increasing mass (FDTABIM) is necessary for the upward causation of the mind-molecule coupling (Figs. 15.17, 15.19), ultimately because force originates at the molecular level and the objects to be moved are at the muscle level. But why is the FDTABIM necessary for the downward causation (Figs. 15.17, 15.20)? In other words, why is it necessary to amplify the molecular processes at the ion channel level to the macroscopic electrical activities at the level of cortical regions such as motor cortex (Fig. 15.20)? One possible answer may be suggested as follows:

Just as the FDTABIM is needed for the upward causation because the force originates at the molecular level in muscle cells and is finally needed at the macroscopic skeletal muscle level (Fig. 15.19), so it may be that the FDTABIM is needed for the downward causation because the control information originates at the molecular level in cortical neurons and the final control information is needed at the level of the macroscopic cortical regions (Fig. 15.20). (15.41)

Statement 15.41 seems reasonable in view of the facts (1) that, just as force generation requires free energy, so does decision making (also called *reasoning*, *computation*, or *selecting* between 0 and 1, between *polarization* and *depolarization*), and (2) that free energy is available only from enzyme-catalyzed chemical reactions or membrane depolarization (i.e., collapsing ion gradients) occurring at the ion channel level.

<sup>aa</sup>Enzymes are molecular machines that are driven by chemical reactions that they catalyze. So the operation of an enzyme can be represented as a trajectory in a phase space (van Gelder and Porter 1995, p. 7) which would collapse when free energy supply is blocked. Therefore, an enzyme in action is a dissipative structure or a *dissipation* and hence can be named as an X-ator, X being the name of the city where the most important research has been done to establish the mechanism of action of the dissipative structure under consideration. In the case of enzymology, there are three research groups, in my opinion, that have made major contributions to advancing our knowledge on how enzymes work – (1) S. Xie (2001) and his group then at the Pacific Northwest National Laboratory, *Richland*, WA (by measuring the single-molecule enzymic activity of cholesterol oxidase analyzed in Sect. 11.3), (2) Rufus Lumry (1974, 2009) and his group at the University of Minnesota at *Minneapolis* (for establishing the role of mechanical processes in enzymic catalysis), and (3) William Jencks (1975) at the Brandies University in *Waltham*, MA, for establishing the fundamental role of the substrate binding processes in enzymic catalysis which he referred to as the *Circe effect*. To acknowledge the contributions made by these three groups, enzymes have been named as *RMWators* in this book (see Fig. 15.16).